Diverse mode of functionalization of ruthenium coordinated β-ketoiminate analogues

Sudip Kumar Bera,[a] Sanjib Panda,[a] Sourajit Dey Baksi,[a] and Goutam Kumar Lahiri*[a]

[a]*Department of Chemistry, Indian Institute of Technology Bombay, Powai, Mumbai 400076, India*

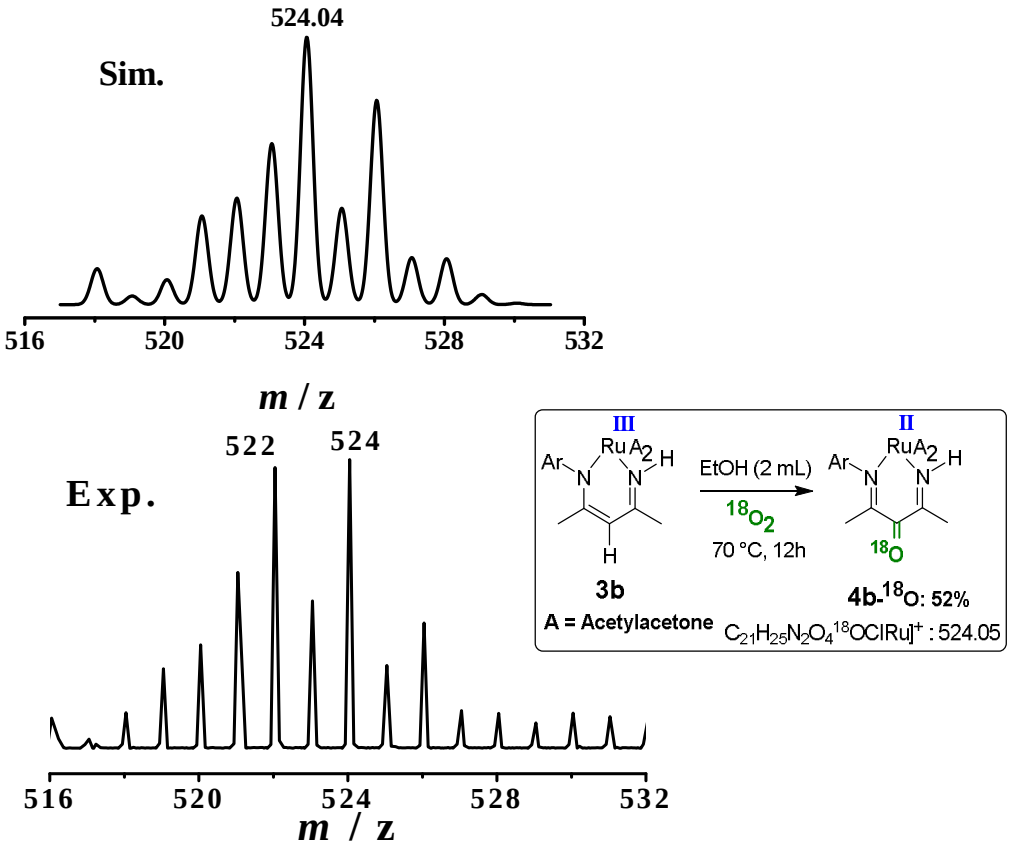

Fig. S1a ESI-MS spectrum of the reaction mixture of **4b** and 18-O labelled **4b** during reaction of [**3b** (0.2 mM) + $^{18}O_2$)] in EtOH. Spectrum was recorded after 12 h of $^{18}O_2$ purging. Peak at m/z = 524 is assigned to {**4b** (^{18}O)}$^+$. Ratio of **4b**-^{18}O:**4b**-^{16}O = 52:48 (Exp.).

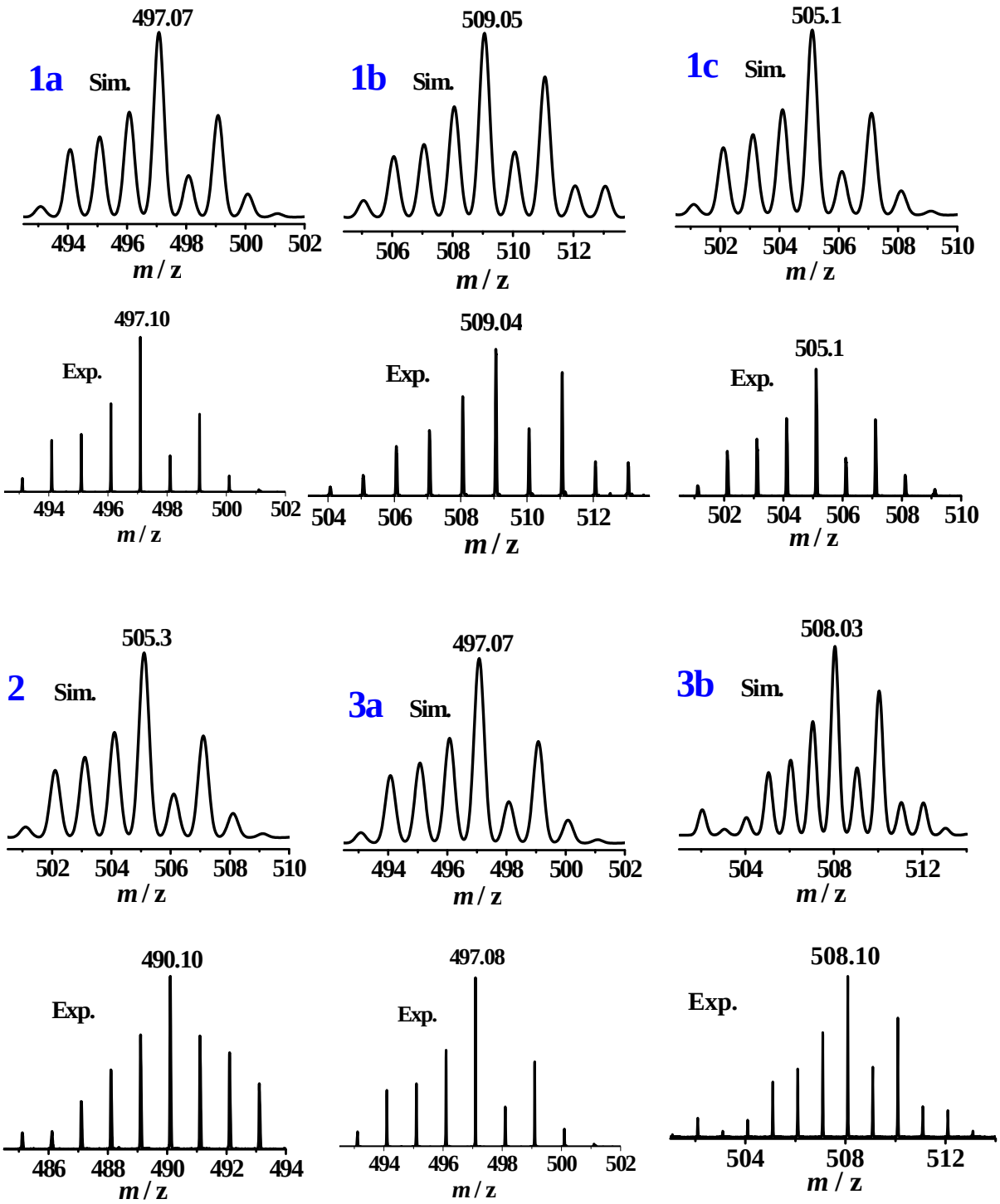

Fig. S1b Experimental and simulated ESI(+) mass spectra of {**1a**+**Na**}$^+$, {**1b**}$^+$, {**1c**}$^+$, {**2**}$^+$, {**3a**+**Na**}$^+$, {**3b**}$^+$ in CH_3CN.

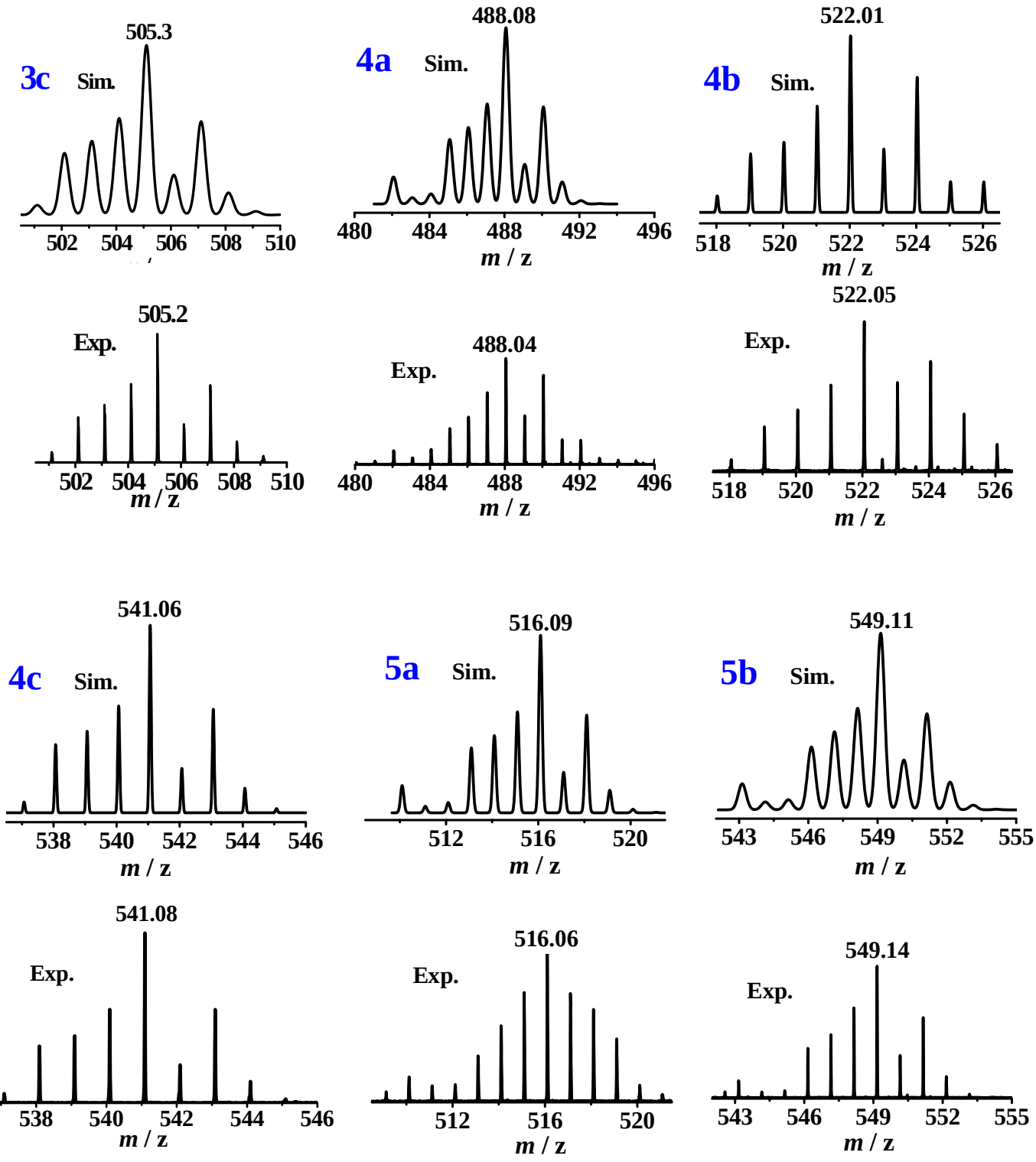

Fig. S1c Experimental and simulated ESI(+) mass spectra of $\{\mathbf{3c}\}^+$, $\{\mathbf{4a}\}^+$, $\{\mathbf{4b}\}^+$,$\{\mathbf{4c+Na}\}^+$,$\{\mathbf{5a+H}\}^+$ and $\{\mathbf{5b}\}^+$ in CH_3CN.

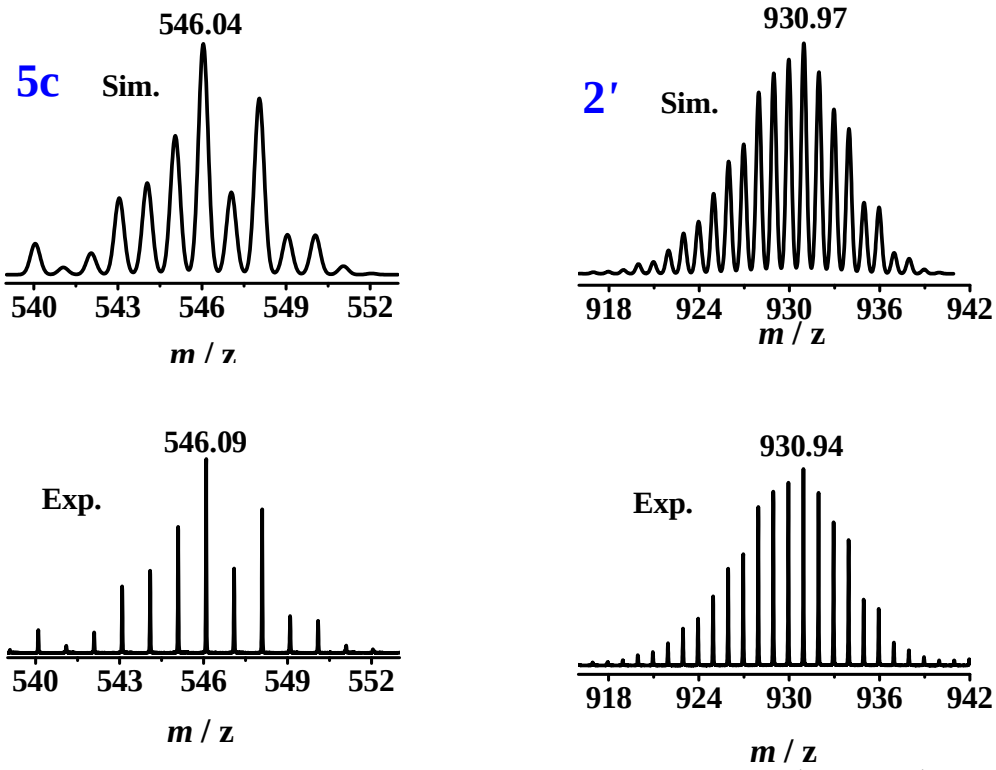

Fig. S1d Experimental and simulated ESI(+) mass spectra of {**5c+H**}$^+$ and {**2′**}$^+$ in CH_3CN.

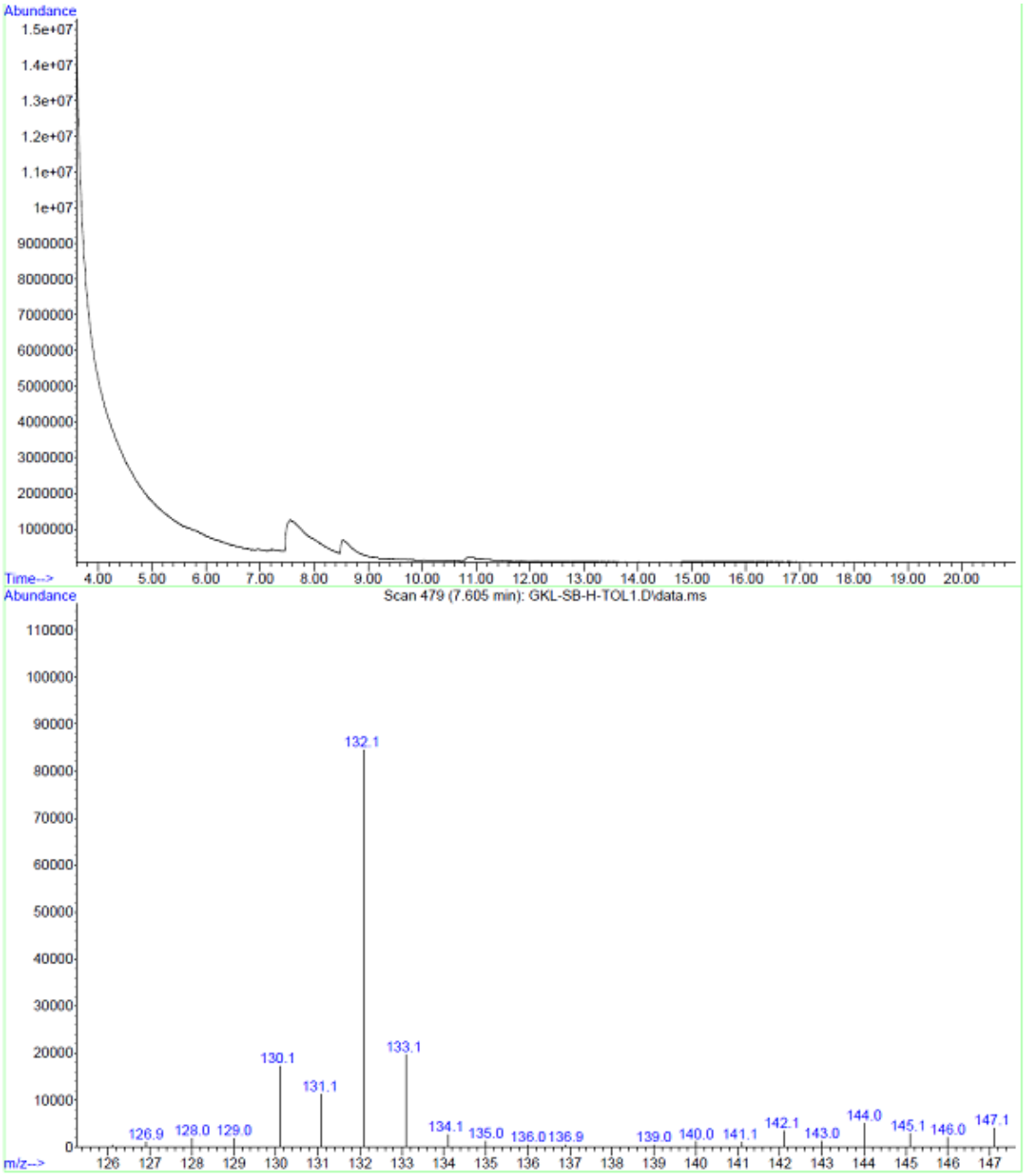

Fig. S1e GC-MS spectra of the intermediate **P** corresponding to **5a** formation in toluene.

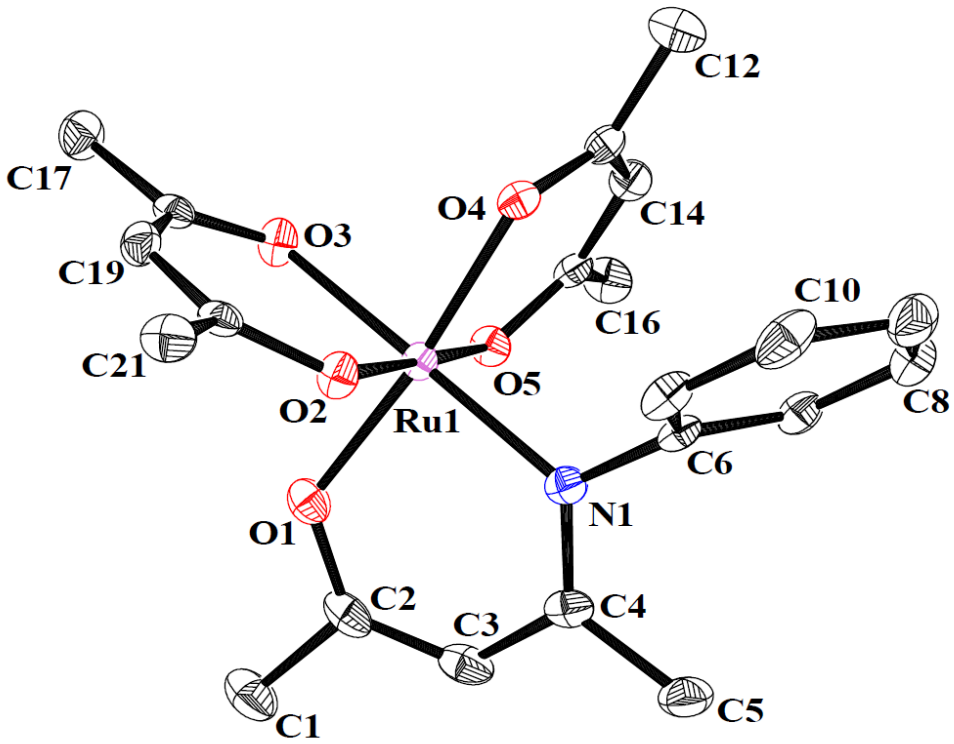

Fig. S2 Perspective view of the asymmetric unit of **1a**. Ellipsoids are drawn at 50% probability level. Hydrogen atoms are omitted for clarity.

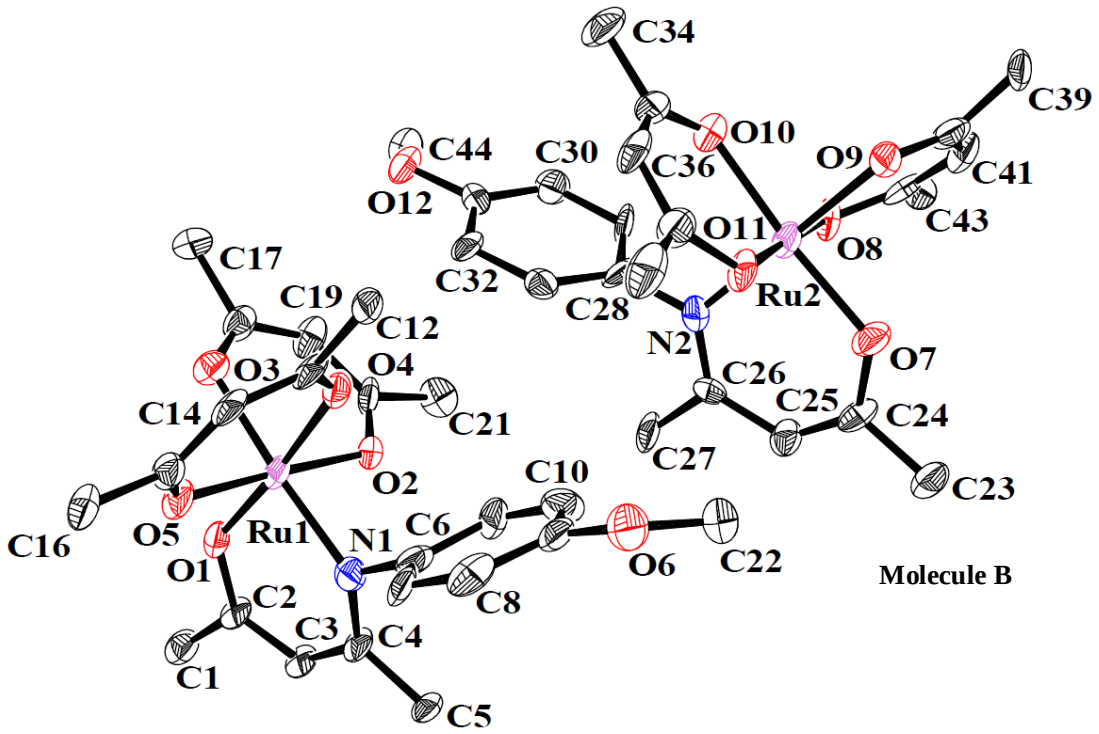

Fig. S3 Perspective view of the asymmetric unit of **1c**, consist of two independent molecules. Ellipsoids are drawn at 50% probability level. Hydrogen atoms are omitted for clarity.

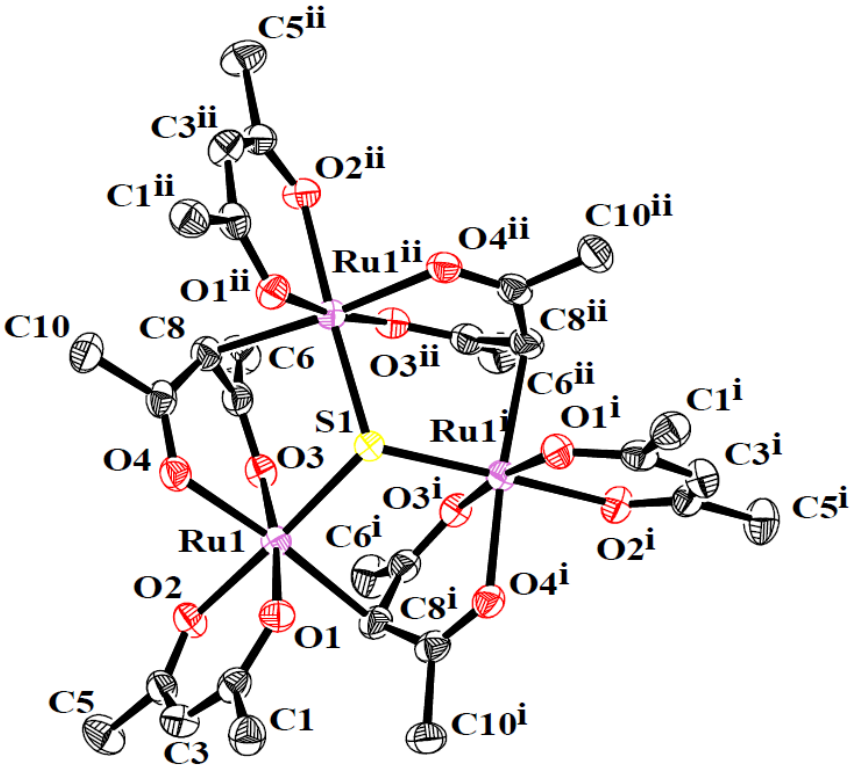

Fig. S4 Perspective view of the asymmetric unit of **2′**. Ellipsoids are drawn at 50%probability level. Hydrogen atoms are omitted for clarity.

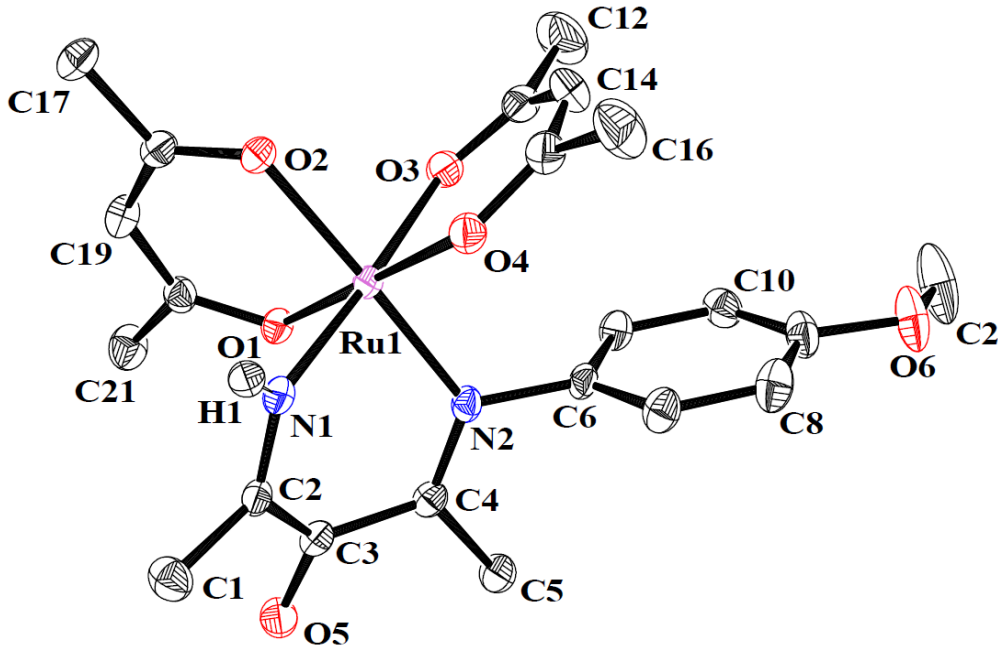

Fig. S5 Perspective view of the asymmetric unit of **4c**. Ellipsoids are drawn at 50% probability level. Hydrogen atoms are omitted for clarity.

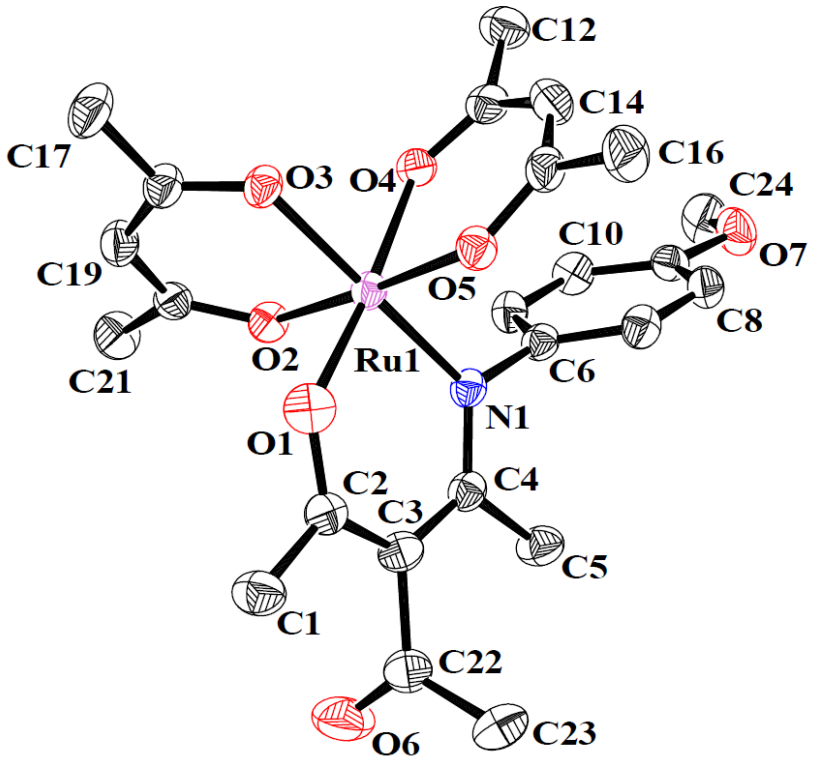

Fig. S6 Perspective view of the asymmetric unit of **5c**. Ellipsoids are drawn at 50% probability level. Hydrogen atoms are omitted for clarity.

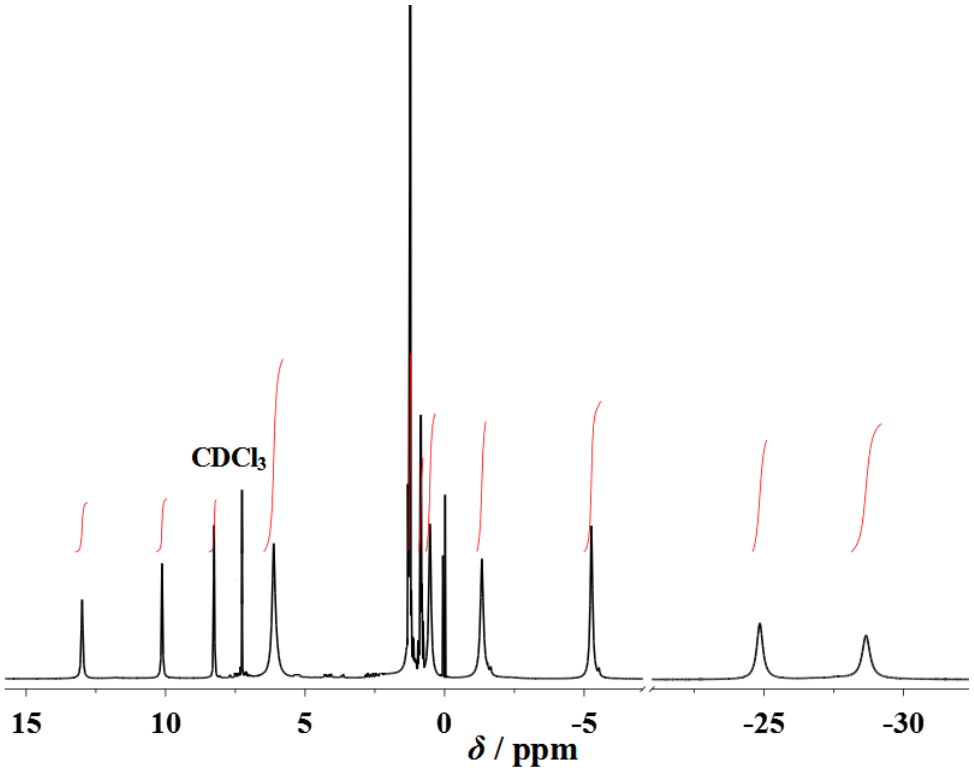

Fig. S7a ^{1}H NMR of **1a** in $CDCl_3$ with TMS (δ = 0 ppm) as internal standard.

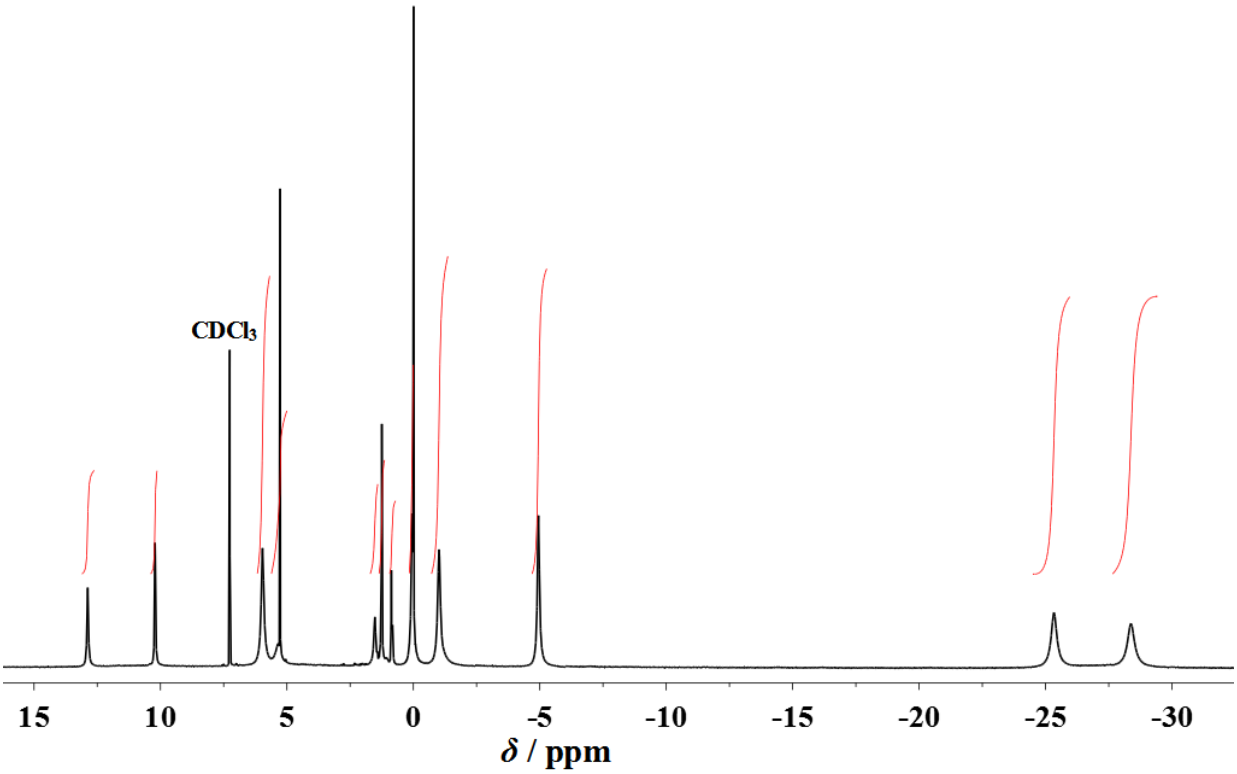

Fig. S7b ^{1}H NMR of **1b** in $CDCl_3$ with TMS (δ = 0 ppm) as internal standard.

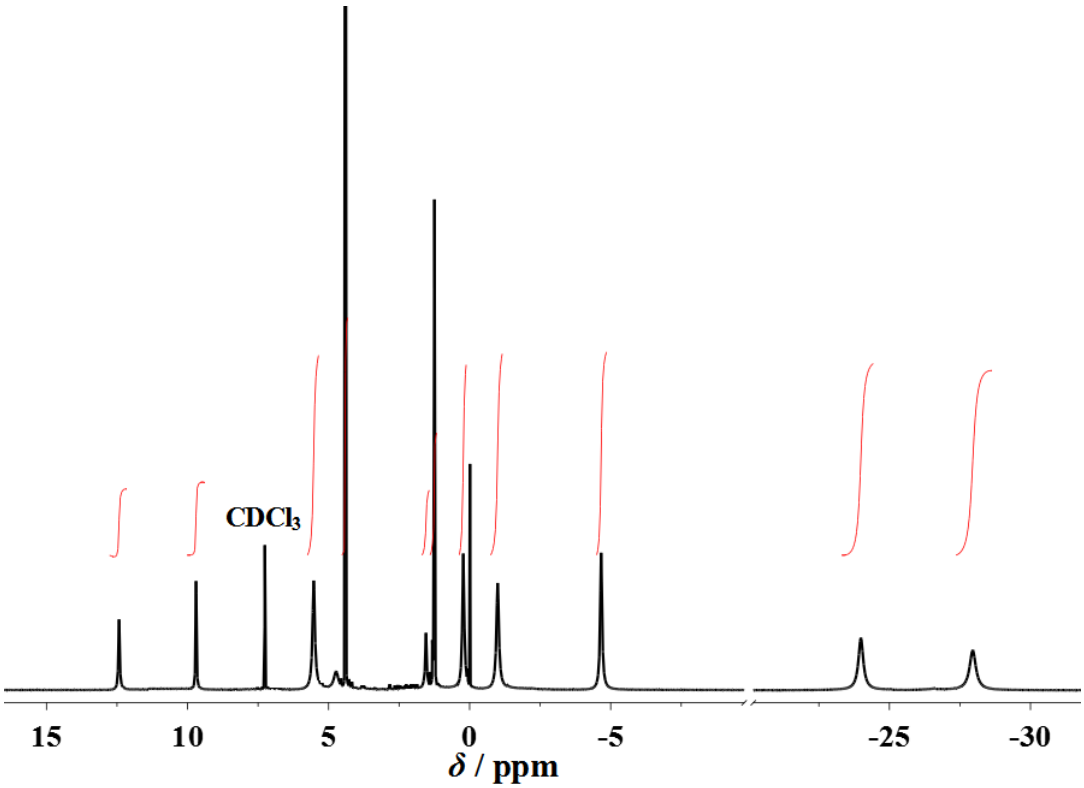

Fig. S7c ^{1}H NMR of **1c** in $CDCl_3$ with TMS (δ = 0 ppm) as internal standard.

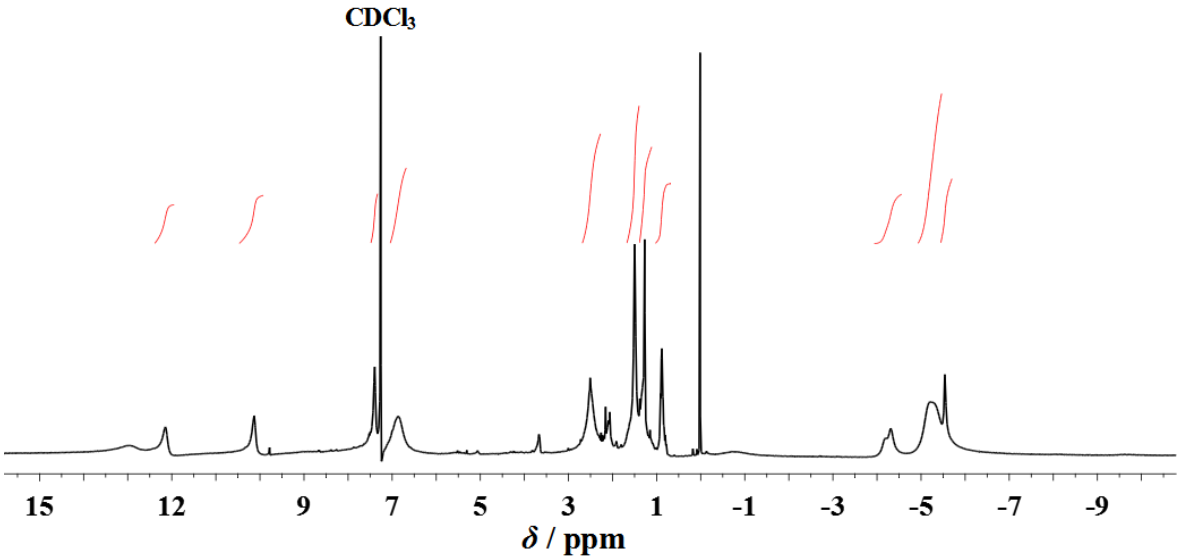

Fig. S7d ^{1}H NMR of **2** in $CDCl_3$ with TMS (δ = 0 ppm) as internal standard.

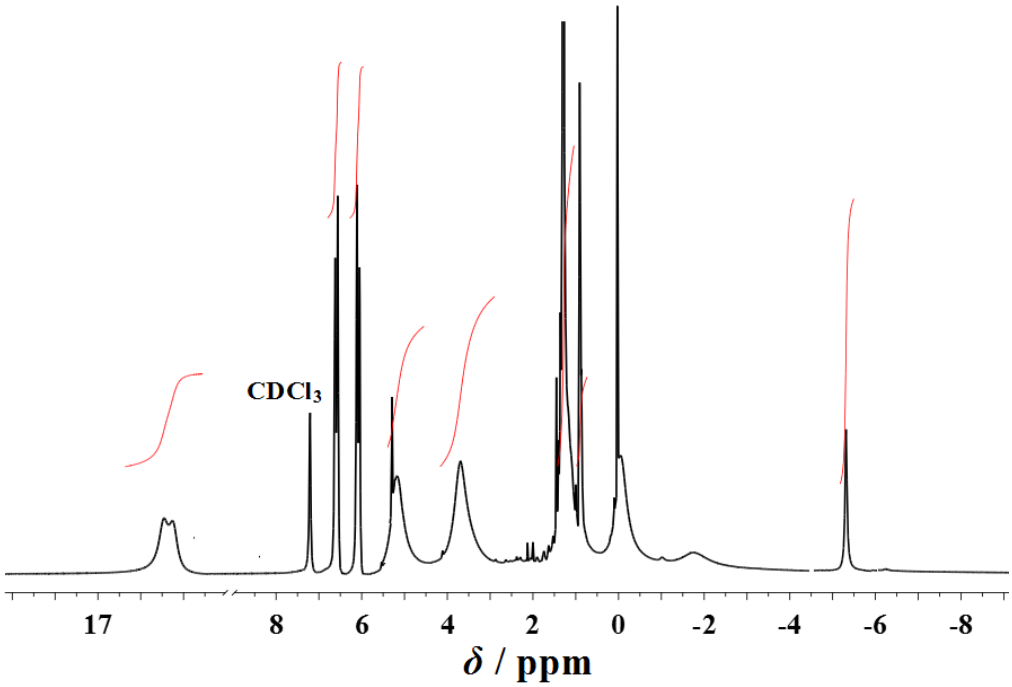

Fig. S7e ^{1}H NMR of **3b** in $CDCl_3$ with TMS (δ = 0 ppm) as internal standard.

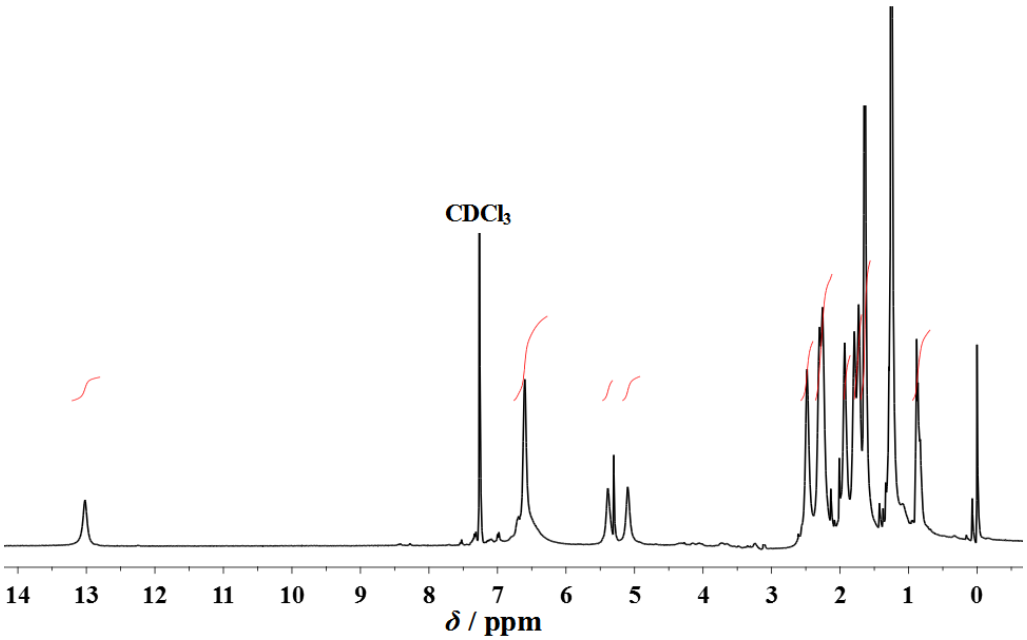

Fig. S7f ^{1}H NMR of **4a** in $CDCl_3$ with TMS (δ = 0 ppm) as internal standard.

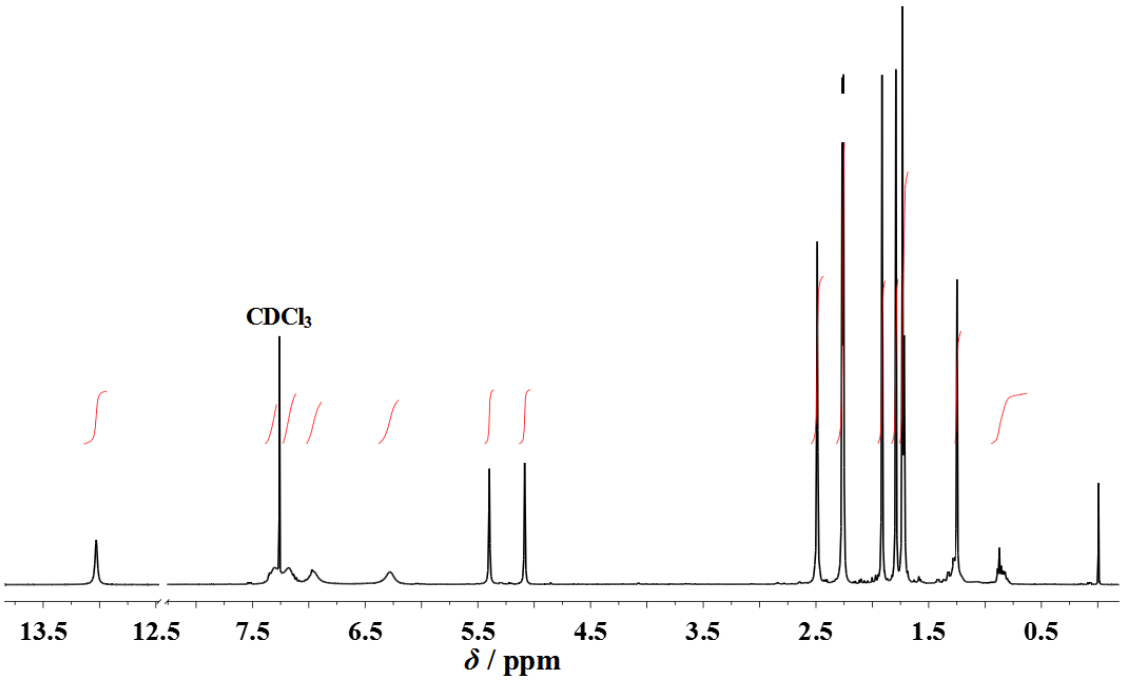

Fig. S7g ^{1}H NMR of **4b** in $CDCl_3$ with TMS (δ = 0 ppm) as internal standard.

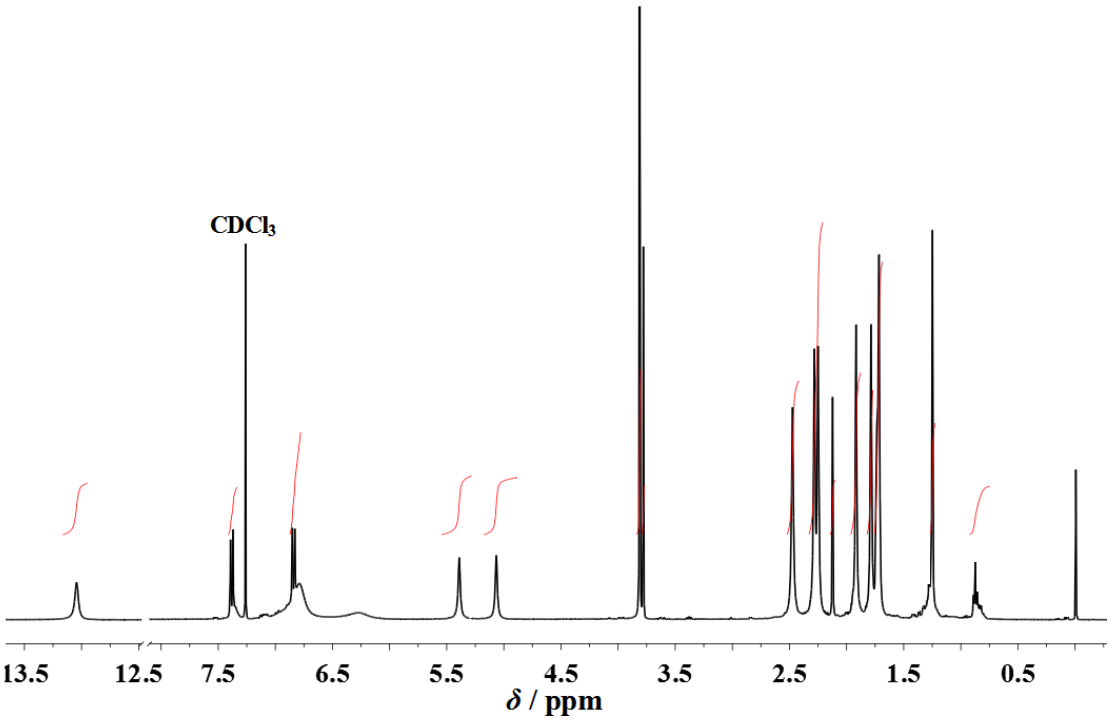

Fig. S7h ^{1}H NMR of **4c** in $CDCl_3$ with TMS (δ = 0 ppm) as internal standard.

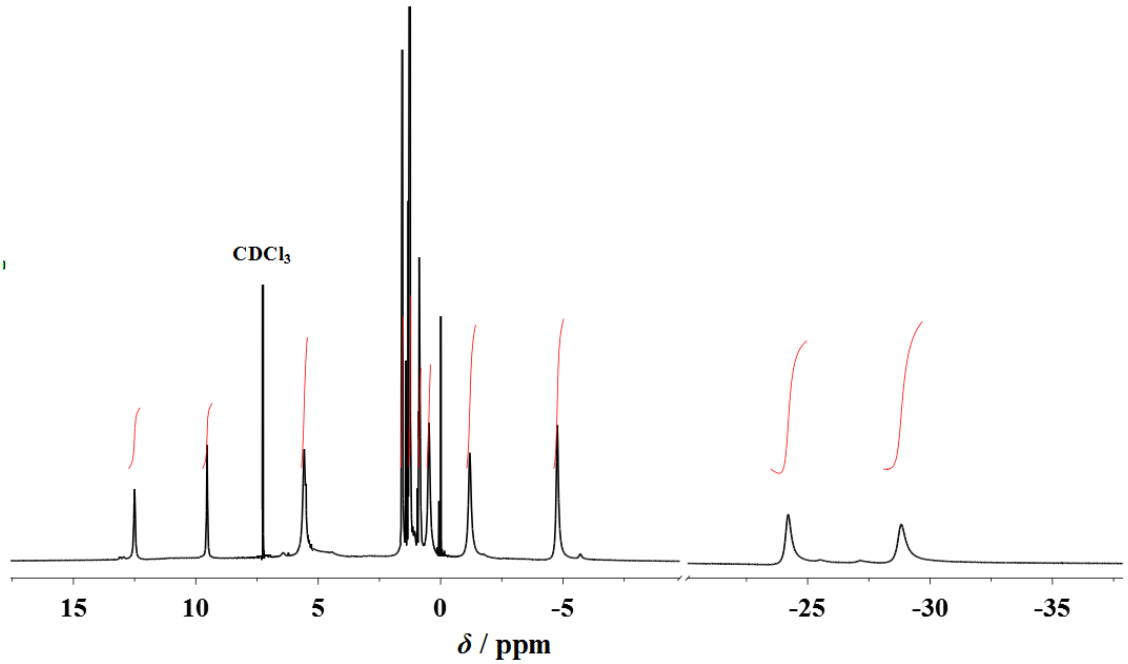

Fig. S7i ^{1}H NMR of **5a** in $CDCl_3$ with TMS (δ = 0 ppm) as internal standard.

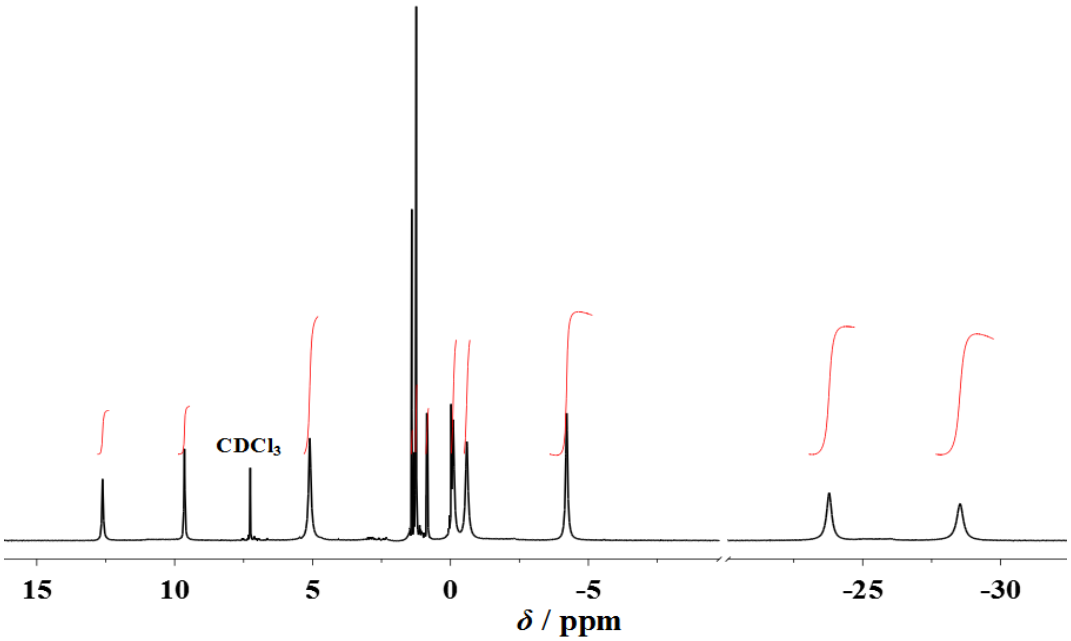

Fig. S7j ^{1}H NMR of **5b** in $CDCl_3$ with TMS (δ = 0 ppm) as internal standard.

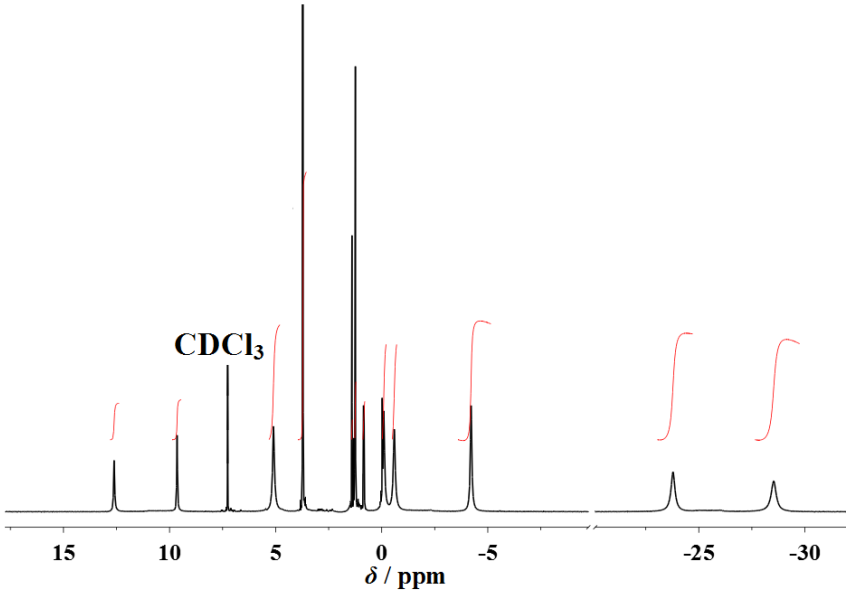

Fig. S7k ^{1}H NMR of **5c** in $CDCl_3$ with TMS (δ = 0 ppm) as internal standard.

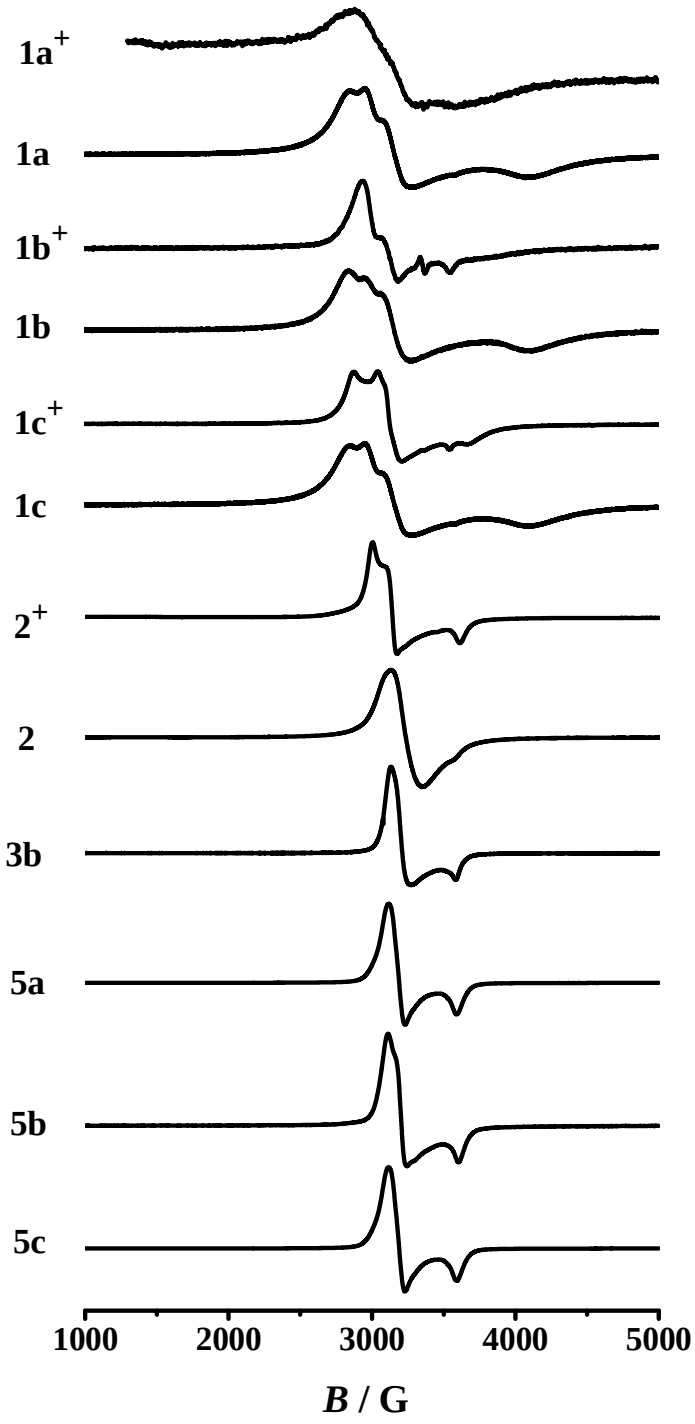

Fig. S8 X-band EPR spectra in CH_2Cl_2/toluene (1:5) at 100 K.

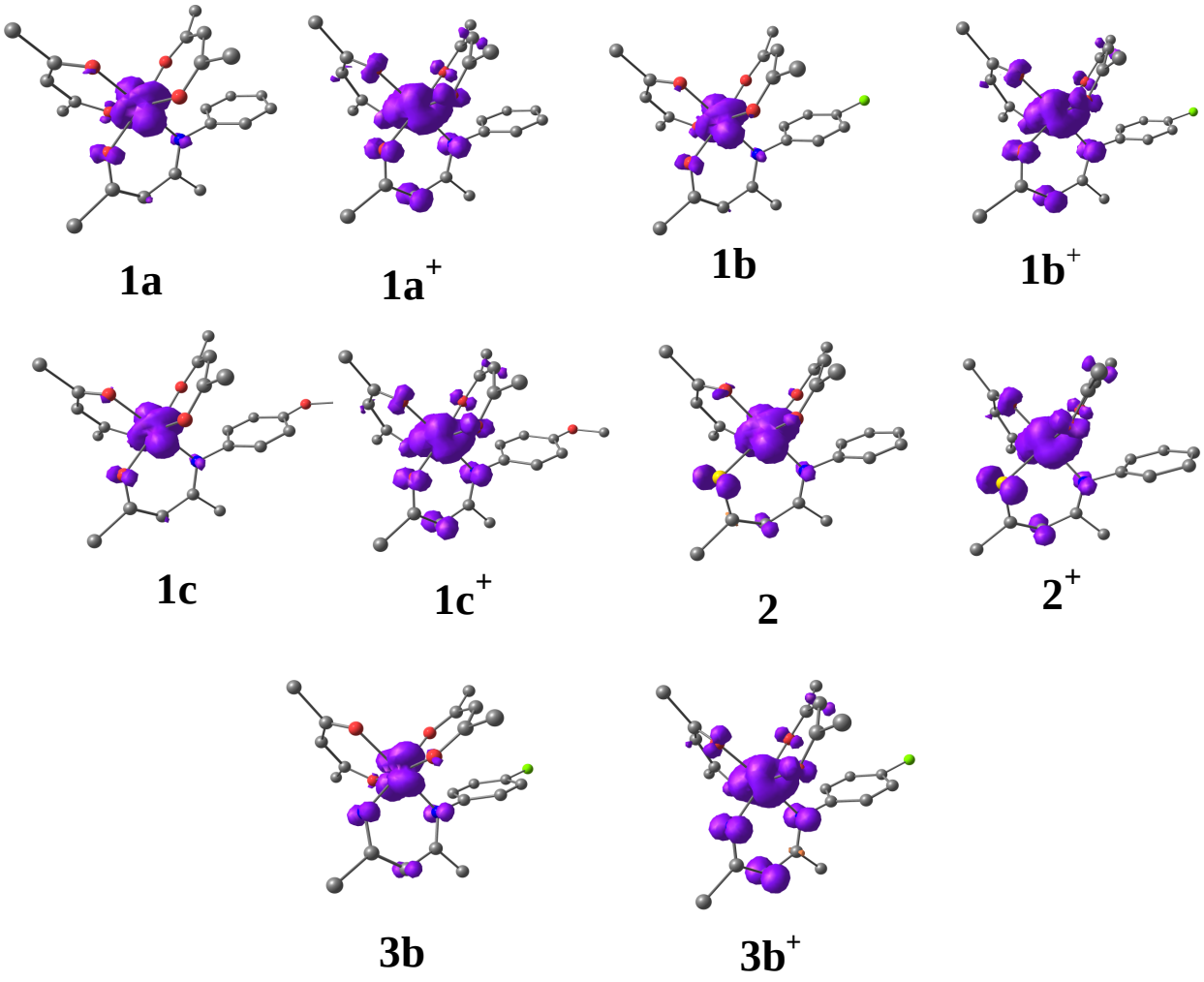

Fig. S9 Mulliken spin density plots of representative complexes.

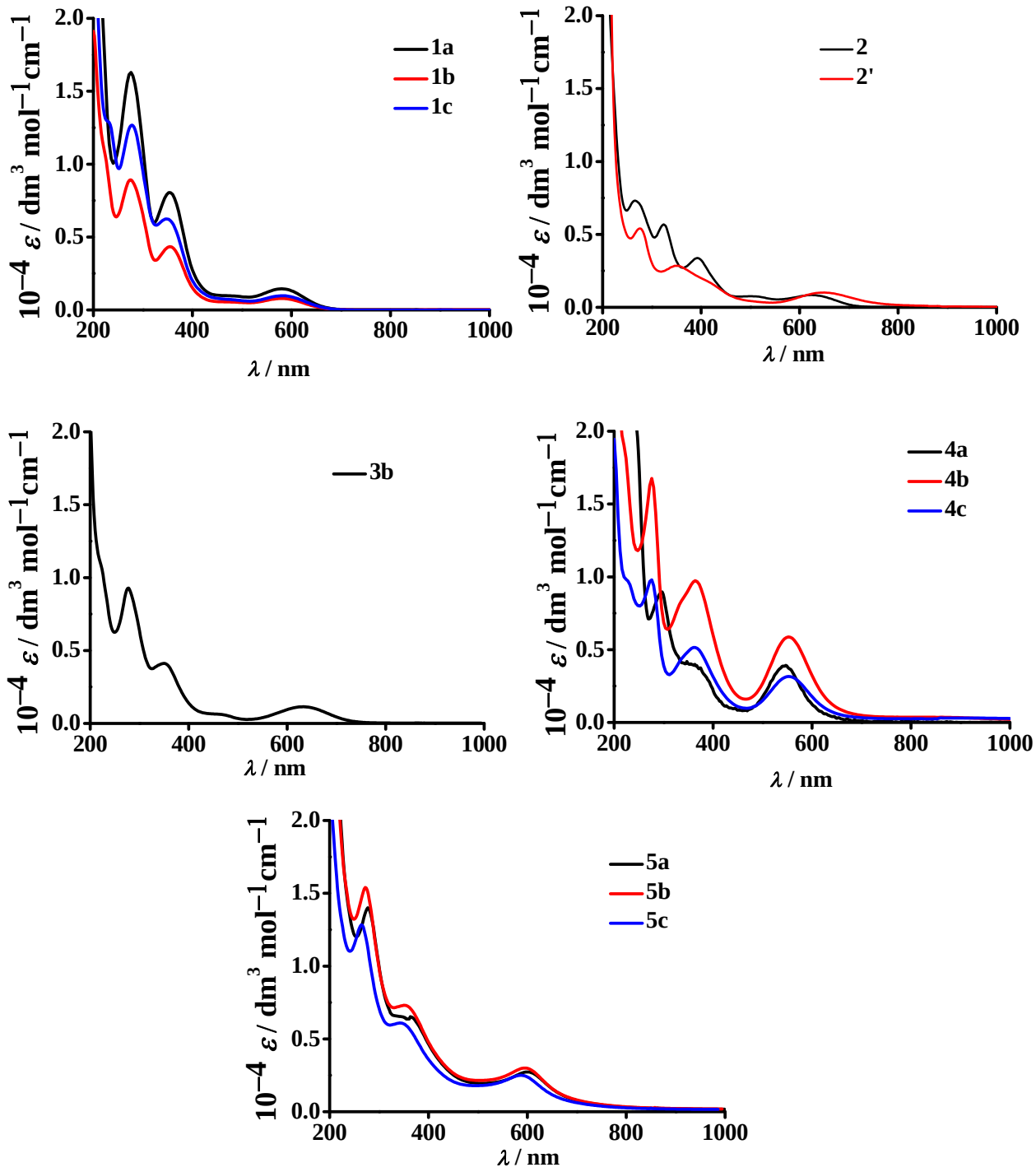

Fig. S10 Electronic spectra of complexes in CH_3CN.

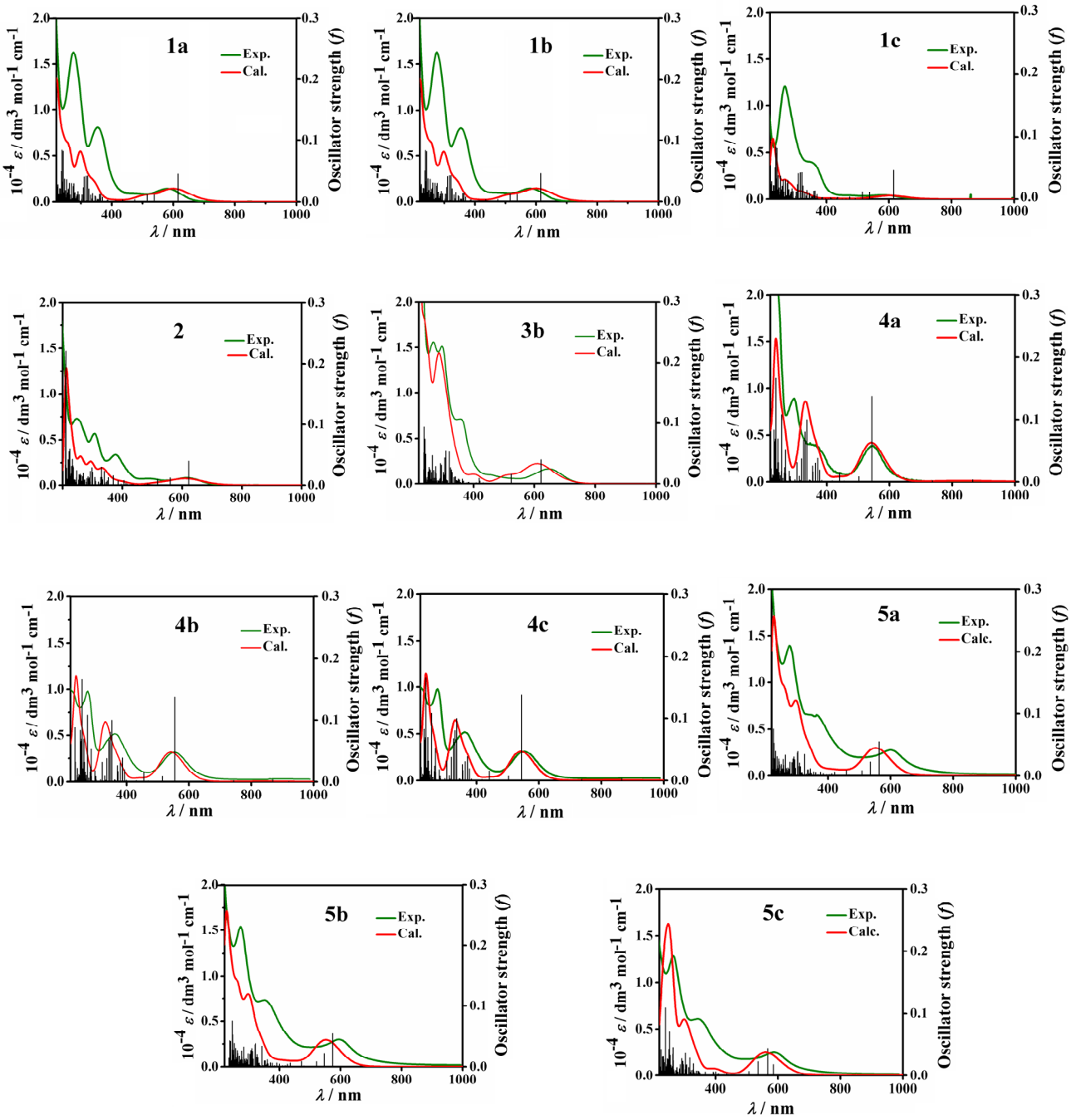

Fig. S11 Experimental (CH_3CN) and TD-DFT ((U)B3LYP/CPCM/CH_3CN) calculated electronic spectra of representative complexes. Oscillator strengths are shown by black vertical lines; the spectra (red) are convoluted with a Gaussian function having full width at half-maximum of 3000 cm^{-1}.

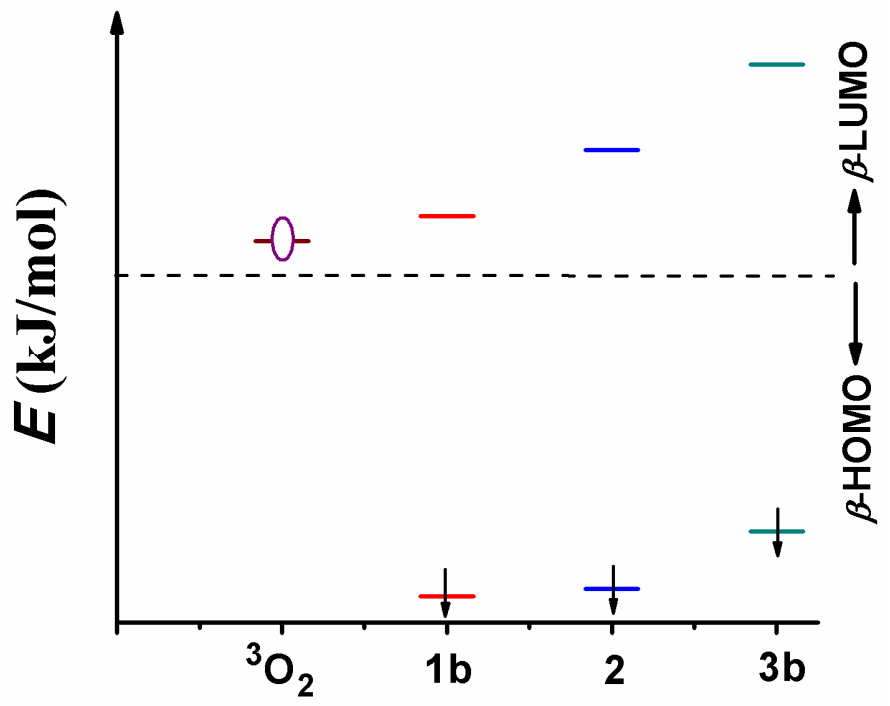

Fig. S12 DFT [(U)B3LYP/LanL2DZ/6-31G*] calculated relative energy level diagram for HOMO of complexes and LUMO of $^3O_2$ (considering HOMO of **1b** as zero).

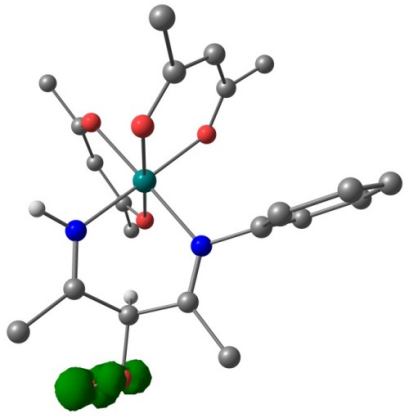

Fig. S13 Mulliken spin density plot of superoxide radical corresponding to **M.**

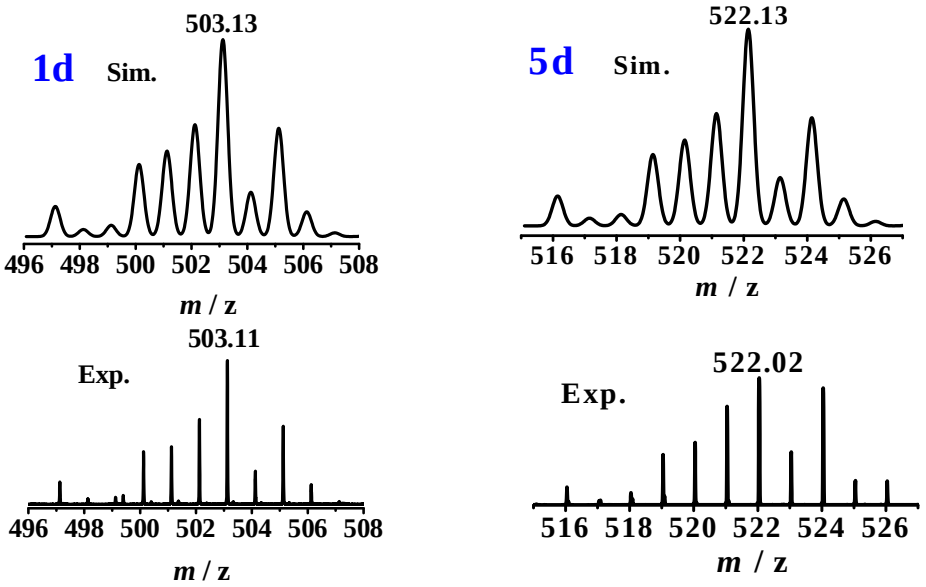

Fig. S14 Experimental and simulated ESI(+) mass spectra of {**1d+Na**}$^{+}$ and {**5d**}$^{+}$ in CH_3CN.

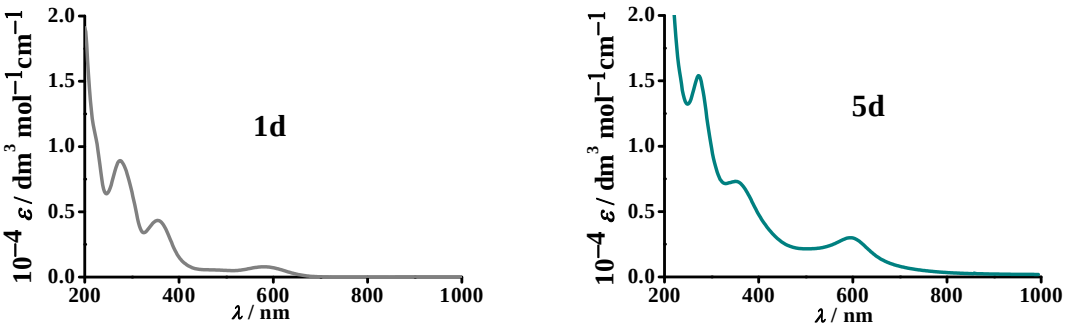

Fig. S15 Electronic spectra of complexes in CH_3CN.

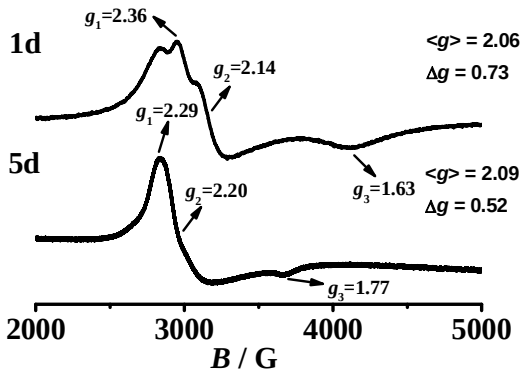

Fig. S16 X-band EPR spectra in CH_2Cl_2/toluene (1:5) at 100 K.

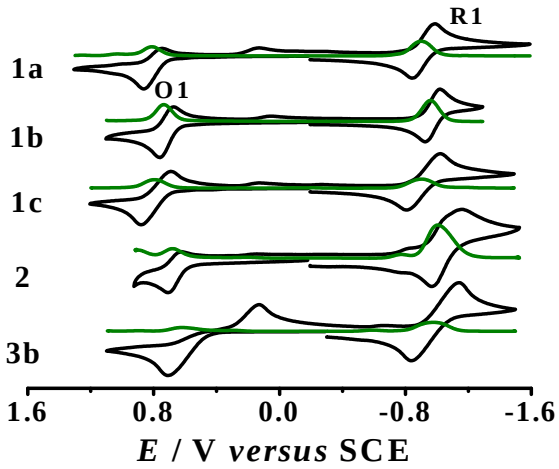

Fig. S17 Cyclic (black) and differential pulse (green) voltammograms in CH_3CN.

Table S1 Selected crystallographic data for complexes **1a**, **1b**, **1c**, **2**, **2′**

complex	**1a**	**1b**	**1c**	**2**	**2'**
empirical formula	$C_{21}H_{26}NO_5Ru$	$C_{21}H_{25}NO_5ClRu$	$C_{44}H_{56}N_2O_{12}Ru_2$	$C_{21}H_{26}NO_4RuS$	$C_{60}H_{84}O_{24}Ru_6S_2$
fw	473.50	507.94	1007.04	489.56	1895.84
crystal system	Monoclinic	Monoclinic	Triclinic	monoclinic	trigonal
space group	*P2₁/c*	*P2₁/c*	*P* $\bar{1}$	*P 1 21/C 1*	*R* $\bar{3}$
a (Å)	8.3726(2)	8.2589(3)	11.3588(12)	8.4297(2)	16.3489(3)
b (Å)	12.5886(4)	12.7453(4)	12.8458(13)	12.4543(3)	16.3489(3)
c (Å)	20.3571(6)	20.9922(5)	15.7582(18)	20.9818(5)	46.9643(9)
α (deg)	90	90	107.603(10)	90	90
β (deg)	90.644(3)	97.68(3)	97.419(9)	99.129(2)	90
γ (deg)	90	90	90.534(8)	90	120
V (Å^3)	2115.32(11)	2189.87(11)	2170.5(4)	2174.89(9)	10871.1(5)
Z	4	4	2	4	6
μ (mm^{-1})	0.771	0.869	0.760	0.842	1.350
T (K)	150(2)	150(2)	150(2)	150(2)	150(2)
D_{calcd} (g cm^{-3})	1.487	1.541	1.541	1.495	1.738
F (000)	972	1036	1036	1004	5700
θ range (deg)	1.91 to 24.998	2.527 to 24.999	1.810 to 24.999	2.558 to 24.996	2.2390 to 31.0520
data/restraints/ parameters	3685 / 0 / 259	3804 / 0 / 268	7658 / 0 / 543	3748 / 0 / 259	4247 / 0 / 294
R1, *w*R2 [*I*> 2*σ*(*I*)]	0.0290, 0.0883	0.0242, 0.0601	0.0946, 0.1932	0.0218, 0.0653	0.0343, 0.0859
R1, *w*R2(all data)	0.0380,0.1102	0.0286, 0.0627	0.1611, 0.2346	0.0236, 0.0672	0.0400, 0.0893
GOF	1.277	1.067	1.078	1.189	1.083
largest diff. peak/hole, (e Å^{-3})	0.931 / -0.999	0.452 / -0.429	0.838/ -1.477	0.331/ -0.338	1.794/-0.723

Table S2 Selected crystallographic data for complexes **3b**, **4b**, **4c**, **5b**, **5c**

complex	**3b**	**4b**	**4c**	**5b**	**5c**
empirical formula	$C_{21}H_{26}ClN_2O_4Ru$	$C_{21}H_{25}ClN_2O_5Ru$	$C_{22}H_{28}N_2O_6Ru$	$C_{23}H_{24}ClNO_6Ru$	$C_{24}H_{30}NO_7Ru$
fw	505.95	521.95	517.53	546.97	544.56
crystal system	triclinic	triclinic	monoclinic	Triclinic	Triclinic
space group	*P* ī	*P* ī	*P 21/n*	*P* ī	*P* ī
a (Å)	9.1225(3)	9.7016(3)	12.4919(4)	9.7720(4)	9.4676(3)
b (Å)	11.0240(4)	11.2609(3)	8.8549(2)	11.2425(4)	11.9575(4)
c (Å)	11.8754	11.3567(3)	22.3944(6)	11.6540(3)	12.7857(3)
α (deg)	90.007(3)	107.004(2)	90	71.213(3)	64.818(3)
β (deg)	107.513(3)	109.034(2)	105.445(3)	85.477(3)	78.619(3)
γ (deg)	102.473(3)	99.357(2)	90	79.983(3)	69.402(3)
V (Å^3)	1109.30(7)	1074.96(6)	2387.69(12)	1193.28(8)	1224.21(7)
Z	2	2	4	2	4
μ (mm^{-1})	0.855	0.896	0.694	0.807	0.683
T (K)	150(2)	150(2)	150(2)	150(2)	150(2)
D_{calcd} (g cm^{-3})	1.515	1.708	1.440	1.5222	1.480
F (000)	516	568	1064.0	554.0688	562
θ range (deg)	1.803 to 25.00	1.973 to 24.998	2.145 to 24.996	1.85 to 24.99	1.763 to 31.206
data/restraints/parameters	3868 / 0/ 272	3784 / 0 / 281	4186 / 0 / 291	3383 / 0 / 295	7250 / 0 / 306
R1, *w*R2 [$I > 2\sigma(I)$]	0.0269, 0.0632	0.0237, 0.0553	0.0265, 0.0621	0.0514, 0.1462	0.0446, 0.1033
R1, *w*R2(all data)	0.0314, 0.0651	0.0273, 0.0567	0.0299, 0.0643	0.0671, 0.1772	0.0621, 0.1228
GOF	1.083	1.045	1.059	1.0343	1.112
largest diff. peak/hole, (e Å^{-3})	0.445/ -0.474	0.443 / -0.722	0.432/ -0.387	0.8939/ -2.0507	0.886/ -1.306

Table S3 Selected experimental and DFT calculated bond lengths (Å) for **1a**, **1b**, **1c**, **5b**, **5c**

bond	**1a**		**1b**		**1c**		**5b**		**5c**	
lengths	X-ray	DFT	X-ray	DFT	X-ray	DFT	X-ray	DFT	X-ray	DFT
Ru1-N1	2.020(3)	2.068	2.0201(16)	2.020	2.022(9)	2.066	2.025(4)	2.077	2.004(2)	2.047
Ru1-O1	1.991(3)	2.013	1.9831(14)	1.983	1.992(7)	2.013	1.973(5)	2.007	1.959(2)	2.036
Ru1-O2	2.023(2)	2.067	2.0004(15)	2.021	1.992(7)	2.040	2.010(4)	2.043	2.0131(19)	2.046
Ru1-O3	2.052(2)	2.077	2.0490(13)	2.049	2.064(7)	2.070	2.039(4)	2.067	2.0482(19)	2.068
Ru1-O4	2.021(2)	2.068	2.0196(13)	2.020	2.029(6)	2.068	2.063(4)	2.053	2.068(2)	2.078
Ru1-O5	2.007(3)	2.040	2.0209(15)	2.000	2.016(7)	2.068	2.043(4)	2.070	2.0367(19)	2.046
C2-O1	1.285(5)	1.289	1.283(3)	1.283	1.274(12)	1.289	1.305(7)	1.288	1.325(4)	1.272
C2-C3	1.381(5)	1.391	1.378(3)	1.378	1.403(14)	1.391	1.421(8)	1.403	1.413(4)	1.430
C3-C4	1.425(5)	1.420	1.412(3)	1.412	1.387(13)	1.420	1.427(7)	1.446	1.395(4)	1.434
C4-N1	1.326(4)	1.325	1.322(2)	1.322	1.334(13)	1.325	1.309(7)	1.321	1.338(4)	1.329
C3-C22							1.491(8)	1.507	1.518(4)	1.490
C22-O6							1.216(8)	1.221	1.200(4)	1.225

Table S4 Selected experimental and DFT calculated bond lengths (Å) for **2, 3b, 4b, 4c**

bond	**2**		**3b**		**4b**		**4c**	
lengths	X-ray	DFT	X-ray	DFT	X-ray	DFT	X-ray	DFT
Ru1-N1	2.0307(17)	2.091	1.956(2)	1.987	1.9460(18)	1.985	1.9484(19)	1.982
Ru1-N2			2.0101(18)	2.058	1.9709(16)	2.045	1.9756(18)	2.045
Ru1-O1	2.0220(14)	2.044	2.0115(15)	2.103	2.0077(14)	2.063	2.0727(15)	2.064
Ru1-O2	2.0620(14)	2.078	2.0375(16)	2.059	2.0301(13)	2.078	2.0161(15)	2.081
Ru1-O3	2.0752(14)	2.101	2.0756(16)	2.110	2.0589(14)	2.098	2.0575(15)	2.100
Ru1-O4	2.0241(14)	2.073	2.0425(15)	2.057	2.0477(14)	2.089	2.0448(15)	2.089
Ru1-S1	2.2392(6)	2.319						
C2-S1	1.695(3)	1.725						
C2-C3	1.356(4)	1.373	1.395(3)	1.402	1.473(3)	1.486	1.476(3)	1.485
C3-C4	1.427(3)	1.437	1.393(3)	1.409	1.480(3)	1.502	1.488(3)	1.502
C4-N1	1.328(3)	1.317						
C2-N1			1.316(3)	1.324	1.290(3)	1.299	1.297(3)	1.299
C4-N2			1.328(3)	1.337	1.306(3)	1.305	1.312(3)	1.305
C3-O5					1.234(3)	1.233	1.246(3)	1.234

Table S5 Selected experimental and DFT calculated bond angles [deg] for **1a**, **1b**, **1c**

bond	**1a**		**1b**		**1c**	
angle [deg]	X-ray	DFT	X-ray	DFT	X-ray	DFT
O(1)-Ru(1)-O(2)	91.36(10)	89.726	88.57(6)	89.739	90.6(3)	89.584
O(1)-Ru(1)-N(1)	93.05(11)	91.250	92.86(6)	91.124	92.5(3)	91.165
O(1)-Ru(1)-O(3)	85.65(10)	87.308	85.31(6)	87.302	88.8(3)	87.345
O(1)-Ru(1)-O(5)	89.05(11)	91.399	90.94(6)	91.449	88.7(3)	91.548
O(2)-Ru(1)-O(4)	87.19(10)	88.913	92.74(6)	88.936	89.1(3)	88.817
N(1)-Ru(1)-O(4)	93.03(10)	93.452	92.96(6)	93.574	92.6(3)	93.591
N(1)-Ru(1)-O(3)	177.15(10)	178.558	176.62(6)	178.423	176.1(3)	178.499
N(1)-Ru(1)-O(5)	90.88(10)	92.82	91.18(6)	92.708	94.4(3)	92.674
N(1)-Ru(1)-O(2)	89.95(10)	88.345	90.07(6)	88.317	83.5(3)	88.417
O(1)-Ru(1)-O(4)	173.65(9)	175.06	174.03(5)	175.079	174.8(3)	174.938
O(3)-Ru(1)-O(4)	88.23(9)	87.990	88.94(5)	88.002	86.0(3)	87.182
O(2)-Ru(1)-O(3)	92.62(9)	91.684	87.05(6)	91.774	92.9(3)	91.757
O(5)-Ru(1)-O(3)	86.56(9)	87.173	91.69(6)	87.235	89.3(3)	87.182
O(5)-Ru(1)-O(2)	179.05(9)	178.357	178.68(5)	178.416	177.7(3)	178.411
O(5)-Ru(1)-O(4)	92.31(10)	89.867	87.62(6)	89.794	91.9(3)	89.962

Table S6 Selected experimental and DFT calculated bond angles [deg] for **5b, 5c, 3b**

bond	**5b**		**5c**		**3b**	
angle [deg]	X-ray	DFT	X-ray	DFT	X-ray	DFT
O(1)-Ru(1)-O(2)	87.43(19)	89.94	90.18(9)	88.663	92.89(6)	90.383
O(1)-Ru(1)-N(1)	87.25(19)	87.84	90.32(10)	86.737	88.07(7)	89.161
O(1)-Ru(1)-O(3)	89.95(17)	88.74	89.23(9)	90.240	87.90(6)	87.246
O(1)-Ru(1)-O(5)	91.86(19)	91.17	91.83(9)	90.314		
O(2)-Ru(1)-O(4)	88.77(17)	88.84	87.80(8)	92.539	85.66(6)	86.858
N(1)-Ru(1)-O(4)	95.37(17)	95.56	93.78(9)	94.800	93.44(7)	89.497
N(1)-Ru(1)-O(3)	176.48(16)	176.57	179.13(7)	176.713	174.41(7)	175.500
N(1)-Ru(1)-O(5)	92.54(18)	92.82	93.02(9)	91.395		
N(1)-Ru(1)-O(2)	87.82(18)	87.88	89.08(9)	90.439	89.05(7)	87.722
N(2)-Ru(1)-O(2)					177.06(6)	177.979
N(2)-Ru(1)-O(4)					91.93(7)	93.721
N(2)-Ru(1)-O(3)					94.42(7)	93.986
N(2)-Ru(1)-O(1)					89.56(7)	89.161
N(1)-Ru(1)-N(2)					89.42(8)	90.347
O(1)-Ru(1)-O(4)	175.30(16)	176.34	175.39(8)	178.039	177.89(6)	175.427
O(3)-Ru(1)-O(4)	87.57(15)	87.85	86.69(8)	88.250	90.50(6)	89.011
O(2)-Ru(1)-O(3)	94.18(16)	92.46	91.66(8)	88.199	87.29(6)	87.958
O(5)-Ru(1)-O(3)	85.42(16)	86.89	86.25(8)	89.911		
O(5)-Ru(1)-O(2)	179.19(13)	178.69	177.09(7)	177.847		
O(5)-Ru(1)-O(4)	91.92(17)	89.99	90.04(8)	88.433		
C(2)-C(3)-C(4)					127.0(2)	127.790

Table S7 Selected experimental and DFT calculated bond angles [deg] for **4b**, **4c**, **2**

bond	**4b**		**4c**		**2**	
angle [deg]	X-ray	DFT	X-ray	DFT	X-ray	DFT
O(1)-Ru(1)-O(2)	94.30(6)	92.607	93.58(6)	92.671	92.08(6)	92.200
O(1)-Ru(1)-N(1)	85.57(7)	84.886	85.90(7)	87.42	90.71(6)	87.741
O(1)-Ru(1)-O(3)	88.25(6)	88.965	89.04(6)	88.906	85.56(6)	86.310
O(2)-Ru(1)-O(4)	84.89(6)	86.438	85.91(6)	86.545	86.74(6)	86.484
N(1)-Ru(1)-O(4)	93.83(7)	93.076	93.55(7)	97.742	90.41(6)	93.768
N(1)-Ru(1)-O(3)	173.27(6)	175.326	174.59(7)	175.128	93.47(6)	93.172
N(1)-Ru(1)-O(2)	91.12(7)	90.895	91.00(7)	90.745	177.07(6)	179.037
N(2)-Ru(1)-O(2)	178.94(6)	177.240	178.23(6)	177.38		
N(2)-Ru(1)-O(4)	94.64(6)	96.075	95.01(7)	95.832		
N(2)-Ru(1)-O(3)	94.26(6)	94.482	94.08(7)	94.829		
N(2)-Ru(1)-O(1)	86.16(6)	84.886	85.49(7)	84.955		
N(1)-Ru(1)-N(2)	87.96(7)	87.834	87.43(8)	88.045		
O(1)-Ru(1)-O(4)	178.98(5)	179.010	179.24(6)	179.199	175.89(6)	175.008
O(3)-Ru(1)-O(4)	92.32(6)	90.178	91.49(6)	90.882	90.42(6)	88.792
O(2)-Ru(1)-O(3)	86.70(6)	86.614	87.41(6)	86.222	85.90(6)	85.903
C(2)-C(3)-C(4)	120.26(18)	121.341	119.66(18)	121.52	131.6(2)	131.068
O(1)-Ru(1)-S(1)					92.96(5)	92.189
O(4)-Ru(1)-S(1)					90.87(5)	92.569
O(3)-Ru(1)-S(1)					171.24(4)	173.343
O(2)-Ru(1)-S(1)					85.52(5)	87.676
N(1)-Ru(1)-S(1)					95.19(5)	93.240

Table S8 EPR data of complexes at 100K

complex	g_1	g_2	g_3	$\langle g \rangle^a$	Δg^b
1a$^+$	2.32	2.15	1.88	2.12	0.44
1a	2.36	2.14	1.64	2.07	0.72
1b$^+$	2.29	2.16	1.88	2.12	0.41
1b	2.35	2.15	1.64	2.07	0.73
1c$^+$	2.33	2.14	1.88	2.12	0.45
1c	2.36	2.14	1.63	2.06	0.73
2$^+$	2.22	2.13	1.85	2.07	0.37
2	2.33	2.14	1.89	2.12	0.44
3b	2.15	2.10	1.87	2.04	0.28
5a	2.14	2.10	1.87	2.04	0.27
5b	2.14	2.10	1.86	2.04	0.28
5c	2.15	2.10	1.87	2.04	0.28

$^a \langle g \rangle = \{(1/3)(g_1^2 + g_2^2 + g_3^2)\}^{1/2}$. $^b \Delta g = g_1 - g_3$

Table S9 DFT calculated (UB3LYP/LanL2DZ/6-31G*) Mulliken spin densities

complex	Ru1	**L**	acac
1a^{+} (*S*=1)	1.211	0.403	0.387
1a (*S*=1/2)	0.807	0.117	0.075
1b^{+} (*S*=1)	1.213	0.386	0.392
1b (*S*=1/2)	0.808	0.115	0.078
1c^{+} (*S*=1)	1.198	0.441	0.361
1c (*S*=1/2)	0.806	0.120	0.072
2^{+} (S=1)	1.192	0.435	0.373
2 (S=1/2)	0.753	0.178	0.069
3b^{+} (S=1)	1.118	0.568	0.314
3b (S=1/2)	0.737	0.219	0.044
5a (*S*=1/2)	0.803	0.110	0.087
5b (*S*=1/2)	0.807	0.117	0.075
5c (*S*=1/2)	0.794	0.130	0.076

Table S10 TD-DFT ((U)B3LYP/CPCM/CH_3CN) calculated electronic transitions for **1a, 1b, 1c, 2, 3b, 4a**

λ/nm expt (DFT)	ε /$M^{-1}cm^{-1}$ (*f*)	transitions	character
1a (*S*=1/2)			
580 (587)	1067 (0.041)	HOMO-2(β)→LUMO(β) (0.94)	L(π)/acac(π)→Ru(dπ)/acac(π*)/L(π*)
350 (353)	7782 (0.041)	HOMO−1(α)→LUMO+1(α) (0.51) HOMO(β)→LUMO+3(β) (0.40)	Ru(dπ)/acac(π)/L(π)→acac(π*)/L(π*) Ru(dπ)/acac(π)/L(π)→acac(π*)/L(π*)
(302)	(0.04)	HOMO−2(α)→LUMO+2(α) (0.51) HOMO−2(α)→LUMO(α) (0.42)	Ru(dπ)/acac(π)/L(π)→L(π*) L(π)/Ru(dπ)/acac(π)→acac(π*)/L(π*)
1b (*S*=1/2)			
581 (604)	1580 (0.045)	HOMO-2(β)→LUMO(β) (0.92)	L(π)/acac(π)→Ru(dπ)/acac(π*)/L(π*)
350 (347)	8195 (0.013)	HOMO−1(α)→LUMO+1(α) (0.41) HOMO(β)→LUMO+3(β) (0.46)	Ru(dπ)/acac(π)/L(π)→acac(π*)/L(π*) Ru(dπ)/acac(π)/L(π)→acac(π*)/L(π*)
1c (*S*=1/2)			
580 (569)	960 (0.02)	HOMO-2(β)→LUMO(β) (0.81)	L(π)/acac(π)→Ru(dπ)/ L(π*)/ acac(π*)
351 (307)	7300(0.014)	HOMO−2(α)→LUMO+1(α) (0.51) HOMO(α)→LUMO+2(α) (0.32)	Ru(dπ)/acac(π)/L(π)→ acac(π*) Ru(dπ)/acac(π)/L(π)→ acac(π*)
(309)	(0.02)	HOMO−2(α)→LUMO(α) (0.57) HOMO−2(α)→LUMO+1(α) (0.33)	Ru(dπ)/acac(π)/L(π)→ L(π*) Ru(dπ)/acac(π)/L(π)→ acac(π*)
2 (*S*=1/2)			
620 (621)	800 (0.04)	HOMO-2(β)→LUMO(β) (0.91)	acac(π)/ L(π)→L(π*)/ Ru(dπ)
393 (369)	5700(0.016)	HOMO−1(α)→LUMO(α) (0.56) HOMO(α)→LUMO+3(α) (0.32)	acac(π)/ Ru(dπ)/L(π)→ acac(π*) L(π)/ Ru(dπ)→ L(π*)/acac(π*)/Ru(dπ)
3b (*S*=1/2)			
650 (658)	1740 (0.06)	HOMO-1(β)→LUMO(β) (0.72)	Ru(dπ)/L(π)/acac(π)→ Ru(dπ)/ L(π*)/ acac(π*)
362 (317)	14400 (0.012)	HOMO−2(β)→LUMO+2(β) (0.53) HOMO−1(α)→LUMO+1(α) (0.38)	L(π)/ acac(π)/→ L(π*)/acac(π*) Ru(dπ)/acac(π)→ L(π*)/acac(π*)
295 (297)	15180 (0.033)	HOMO−2(α)→LUMO+1(α) (0.56) HOMO−2(β)→LUMO+2(β) (0.33)	Ru(dπ)/L(π)→ L(π*)/acac(π*) Ru(dπ)/L(π)→ L(π*)/acac(π*)
4a (*S*=0)			
553 (543)	3185 (0.137)	HOMO→LUMO (0.51) HOMO−2→LUMO (0.23)	Ru(dπ)/L(π)/acac(π)→L(π*)/ Ru(dπ) Ru(dπ)/L(π)→ L(π*)/ Ru(dπ)
362 (354)	5166 (0.025)	HOMO−1→LUMO+2 (0.53)	Ru(dπ)/acac(π)/L(π)→ acac(π*)/L(π*)

Table S11 TD-DFT ((U)B3LYP/CPCM/CH_3CN) calculated electronic transitions for **4b, 4c, 5a, 5b** and **5c**

λ/nm expt (DFT)	ε /$M^{-1}cm^{-1}$ (*f*)	transitions	character
4b (*S*=0)			
553 (543)	3185 (0.137)	HOMO→LUMO (0.51) HOMO−2→LUMO (0.23)	Ru(dπ)/L(π)/acac(π)→L(π*)/ Ru(dπ) Ru(dπ)/L(π)→ L(π*)/ Ru(dπ)
362 (354)	5166 (0.025)	HOMO−1→LUMO+2 (0.53)	Ru(dπ)/acac(π)/L(π)→ acac(π*)/L(π*)
4c (S=0)			
550 (541)	3185 (0.137)	HOMO→LUMO (0.51) HOMO−2→LUMO (0.23)	Ru(dπ)/L(π)/acac(π)→L(π*)/ Ru(dπ) Ru(dπ)/L(π)→ L(π*)/ Ru(dπ)
362 (351)	5166 (0.025)	HOMO−1→LUMO+2 (0.53)	Ru(dπ)/acac(π)/L(π)→ acac(π*)/L(π*)
5a (S=1/2)			
591 (564)	3060 (0.054)	HOMO-2(β)→LUMO(β) (0.85)	L(π)/acac(π)→Ru(dπ)/ L(π*)/ acac(π*)
351 (307)	7300(0.014)	HOMO−2(α)→LUMO+1(α) (0.41) HOMO−2(α)→LUMO+2(α) (0.32)	Ru(dπ)/acac(π)/L(π)→ acac(π*) Ru(dπ)/acac(π)/L(π)→ acac(π*)
5b (S=1/2)			
591 (563)	3060 (0.054)	HOMO-2(β)→LUMO(β) (0.85)	L(π)/acac(π)→Ru(dπ)/ L(π*)/ acac(π*)
351 (307)	7300(0.014)	HOMO−2(α)→LUMO+1(α) (0.41) HOMO−2(α)→LUMO+2(α) (0.32)	Ru(dπ)/acac(π)/L(π)→ acac(π*) Ru(dπ)/acac(π)/L(π)→ acac(π*)
5c (S=1/2)			
591 (563)	3060 (0.054)	HOMO-2(β)→LUMO(β) (0.85)	L(π)/acac(π)→Ru(dπ)/ L(π*)/ acac(π*)
351 (307)	7300(0.014)	HOMO−2(α)→LUMO+1(α) (0.41) HOMO−2(α)→LUMO+2(α) (0.32)	Ru(dπ)/acac(π)/L(π)→ acac(π*) Ru(dπ)/acac(π)/L(π)→ acac(π*)

Table S12 Electrochemical data

Complexes	E^0[V] (ΔE_p[mV])[a,b]	
	O1	R1
1a	0.99 (110)	–0.72 (120)
1b	1.04 (100)	–0.65 (120)
1c	0.97 (160)	–0.72 (200)
2	0.805 (70)	–0.80 (120)
3b	0.43[c]	–0.99 (300)

[a]From cyclic voltammetry in CH_3CN/0.1 M Et_4NClO_4, scan rate 100 mV s^{-1}.

[b]Potential in V versus SCE; peak potential differences ΔE_p/mV (in parentheses).

[c]Irreversible.

Table S13 Composition and energies of selected molecular orbitals of **1a** (*S*=1/2)

MO	energy (eV)	% composition		
		Ru	L^-	$acac^-$
		α-spin		
HOMO–5	–6.364	14	61	24
HOMO–4	–6.225	27	31	43
HOMO–3	–5.883	3	30	67
HOMO–2	–5.488	72	9	18
HOMO–1	–5.076	41	25	34
SOMO	–5.071	46	28	26
LUMO	–0.601	3	8	88
LUMO+1	–0.522	2	40	58
LUMO+2	–0.499	7	52	41
LUMO+3	0.002	74	14	12
LUMO+4	0.165	2	93	5
LUMO+5	0.493	50	13	37
		β–spin		
HOMO–5	–6.341	4	77	19
HOMO–4	–6.138	26	12	63
HOMO–3	–6.015	12	20	68
HOMO–2	–5.649	6	66	28
HOMO–1	–5.123	72	11	17
SOMO	–4.829	60	9	31
LUMO	–2.332	66	16	18
LUMO+1	–0.564	4	18	79
LUMO+2	–0.460	5	18	79
LUMO+3	–0.437	7	16	77
LUMO+4	0.066	9	83	8
LUMO+5	0.173	2	93	5

α-spin			
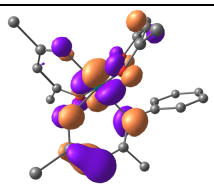	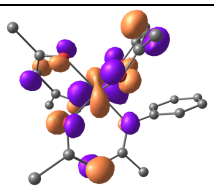	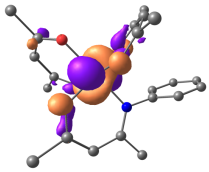	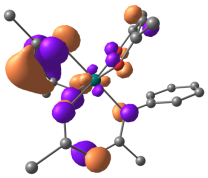
SOMO	HOMO–1	HOMO–2	HOMO–3
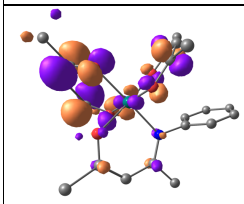	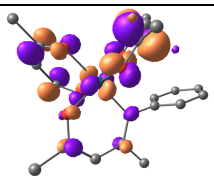	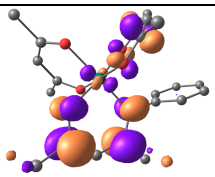	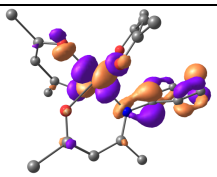
LUMO	LUMO+1	LUMO+2	LUMO+3
β-spin			
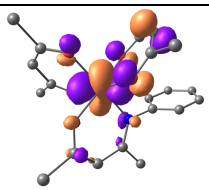	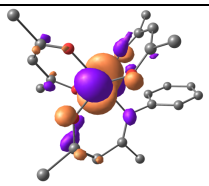	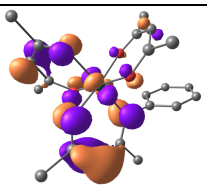	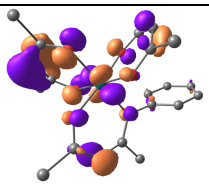
SOMO	HOMO–1	HOMO–2	HOMO–3
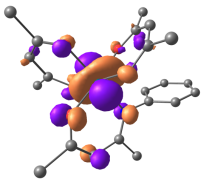	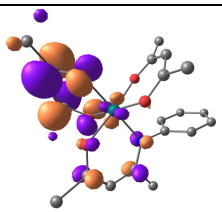	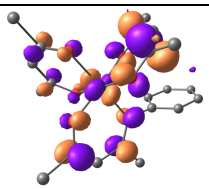	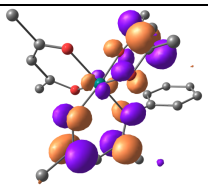
LUMO	LUMO+1	LUMO+2	LUMO+3

Table S14 Composition and energies of selected molecular orbitals of **1b** (*S*=1/2)

MO	energy (eV)	% composition		
		Ru	L^-	$acac^-$
		α-spin		
HOMO–5	–6.532	33	32	35
HOMO–4	–6.270	10	70	19
HOMO–3	–6.038	5	23	73
HOMO–2	–5.832	73	10	18
HOMO–1	–5.370	33	34	33
SOMO	–5.359	45	24	31
LUMO	–0.906	4	17	79
LUMO+1	–0.856	9	71	20
LUMO+2	–0.828	3	87	11
LUMO+3	–0.433	22	62	16
LUMO+4	– 0.279	5	88	6
LUMO+5	– 0.168	47	20	33
		β–spin		
HOMO–5	–6.418	19	47	34
HOMO–4	–6.267	12	45	43
HOMO–3	–6.134	15	31	54
HOMO–2	–5.830	9	55	37
HOMO–1	–5.477	72	13	14
SOMO	–5.127	56	11	33
LUMO	–2.699	67	16	17
LUMO+1	–0.870	3	28	69
LUMO+2	–0.800	8	57	34
LUMO+3	–0.768	4	15	81
LUMO+4	–0.328	15	76	9
LUMO+5	– 0.270	1	95	4

α-spin			
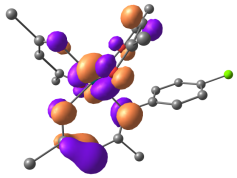	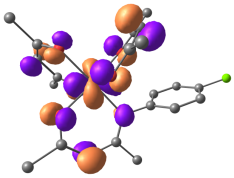	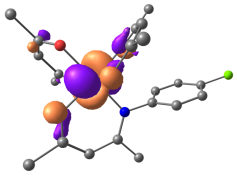	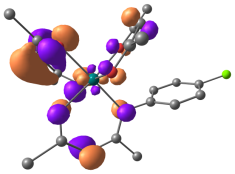
SOMO	HOMO−1	HOMO−2	HOMO−3
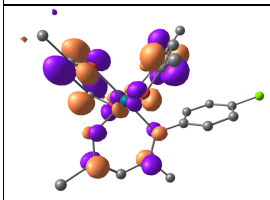	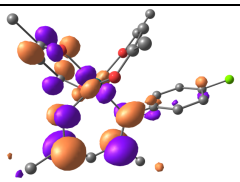	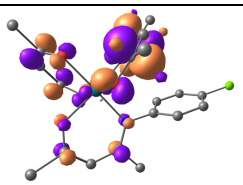	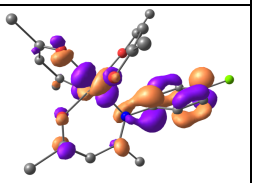
LUMO	LUMO+1	LUMO+2	LUMO+3
β-spin			
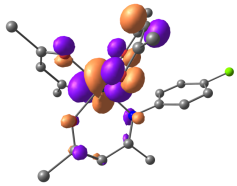	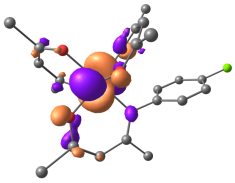	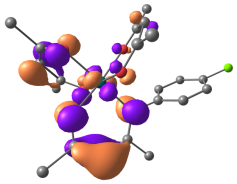	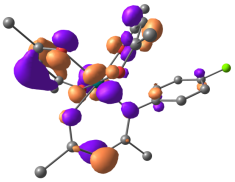
SOMO	HOMO−1	HOMO−2	HOMO−3
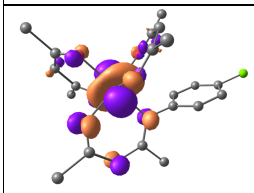	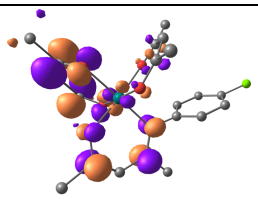	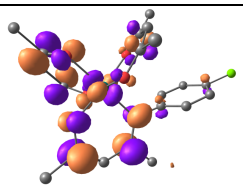	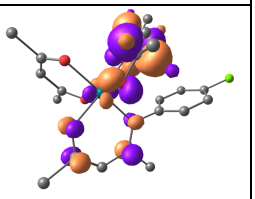
LUMO	LUMO+1	LUMO+2	LUMO+3

Table S15 Composition and energies of selected molecular orbitals of **1c** (*S*=1/2)

MO	energy (eV)	% composition		
		Ru	L^-	$acac^-$
		α-spin		
HOMO–5	–6.369	39	21	40
HOMO–4	–5.921	6	23	71
HOMO–3	–5.792	28	54	17
HOMO–2	–5.650	54	33	13
HOMO–1	–5.234	45	10	45
SOMO	–5.213	34	51	15
LUMO	–0.793	4	8	88
LUMO+1	–0.721	4	3	92
LUMO+2	–0.681	6	87	7
LUMO+3	–0.111	43	25	32
LUMO+4	– 0.031	25	62	14
LUMO+5	0.026	23	62	15
		β–spin		
HOMO–5	–6.240	29	14	58
HOMO–4	–6.046	13	24	62
HOMO–3	–5.750	4	79	17
HOMO–2	–5.688	12	59	29
HOMO–1	–5.323	70	17	13
SOMO	–4.990	57	11	32
LUMO	–2.560	67	16	17
LUMO+1	–0.752	3	14	83
LUMO+2	–0.665	6	5	89
LUMO+3	–0.626	6	81	13
LUMO+4	–0.002	1	95	4
LUMO+5	0.110	31	51	18

α-spin			
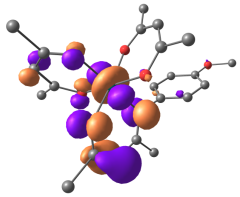	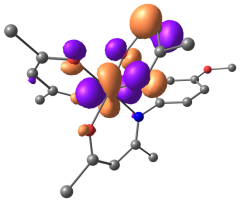	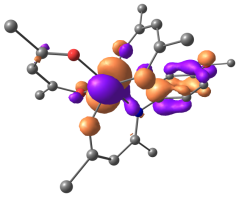	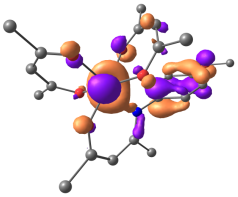
SOMO	HOMO−1	HOMO−2	HOMO−3
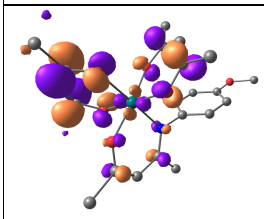	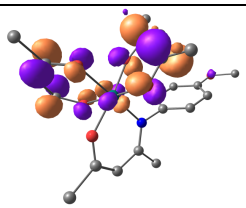	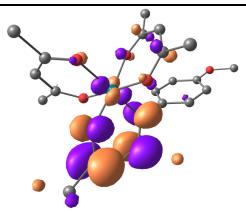	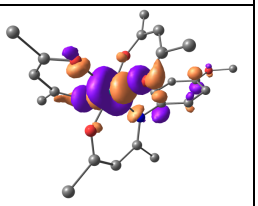
LUMO	LUMO+1	LUMO+2	LUMO+3
β-spin			
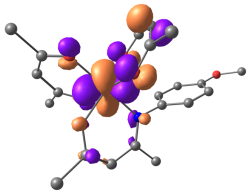	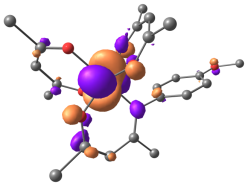	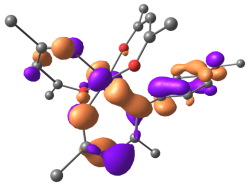	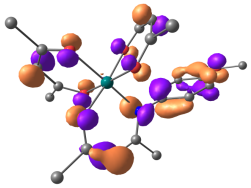
SOMO	HOMO−1	HOMO−2	HOMO−3
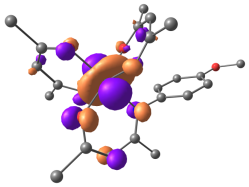	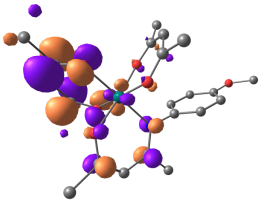	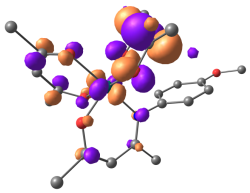	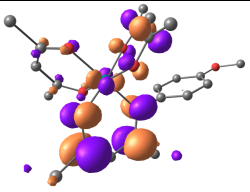
LUMO	LUMO+1	LUMO+2	LUMO+3

Table S16 Composition and energies of selected molecular orbitals of **1b**$^{+}$ (*S*=1)

MO	energy (eV)	% composition		
		Ru	L^{-}	$acac^{-}$
		α-spin		
HOMO–5	–10.437	67	9	23
HOMO–4	–10.006	23	24	52
HOMO–3	–9.821	35	22	43
HOMO–2	–9.675	0	100	1
HOMO–1	–9.621	16	44	40
HOMO	–9.30	6	86	8
LUMO	–4.603	52	10	38
LUMO+1	–4.521	37	44	19
LUMO+2	–4.435	5	50	44
LUMO+3	–4.290	19	20	61
LUMO+4	–4.173	8	13	79
LUMO+5	–2.972	1	96	3
		β–spin		
HOMO–5	–10.111	39	19	42
HOMO–4	–10.018	23	37	40
HOMO–3	–9.829	45	27	28
HOMO–2	–9.617	36	19	45
HOMO–1	–9.602	4	33	63
HOMO	–9.440	4	90	6
LUMO	–7.391	62	12	26
LUMO+1	–7.099	54	28	18

α-spin			
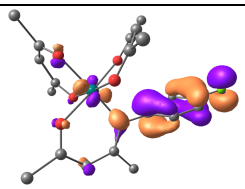	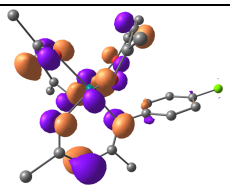	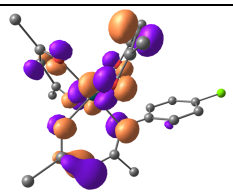	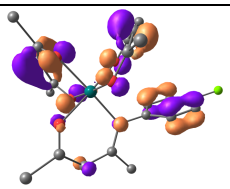
HOMO	HOMO−1	HOMO−2	HOMO−3
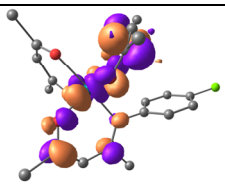	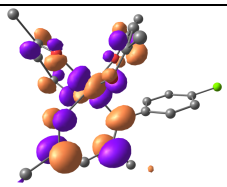	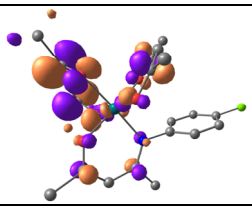	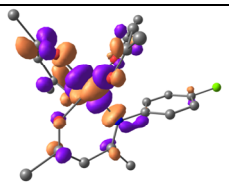
LUMO	LUMO+1	LUMO+2	LUMO+3
β-spin			
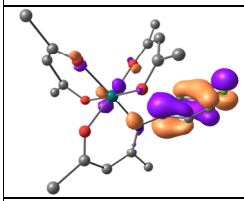	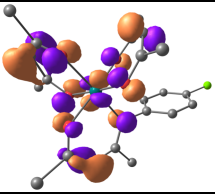	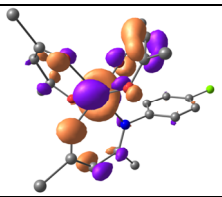	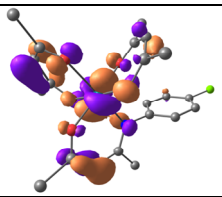
HOMO	HOMO−1	HOMO−2	HOMO−3
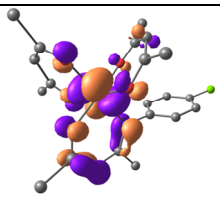	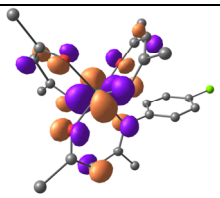	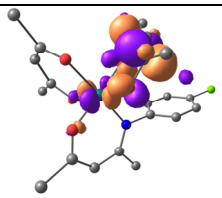	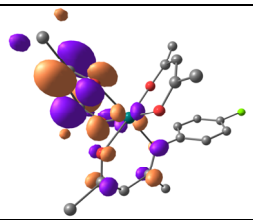
LUMO	LUMO+1	LUMO+2	LUMO+3

Table S17 Composition and energies of selected molecular orbitals of **1b**$^{-}$ (*S*=0)

MO	energy (eV)	% composition		
		Ru	L^{-}	$acac^{-}$
HOMO–5	–2.238	14	13	73
HOMO–4	–2.181	11	10	79
HOMO–3	–1.829	5	68	27
HOMO–2	–0.344	72	10	18
HOMO–1	–0.156	70	10	19
HOMO	0.220	66	18	17
LUMO	3.143	1	93	6
LUMO+1	3.224	2	94	4
LUMO+2	3.282	4	12	84
LUMO+3	3.361	4	21	75
LUMO+4	3.634	11	68	21
LUMO+5	4.321	70	12	18

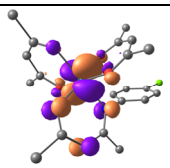	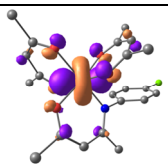	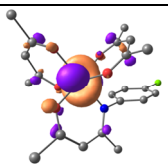	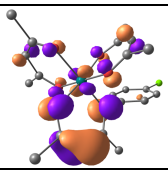
HOMO	HOMO–1	HOMO–2	HOMO–3
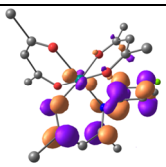	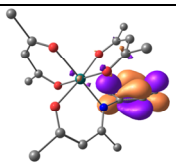	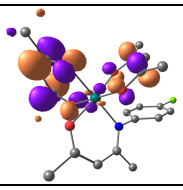	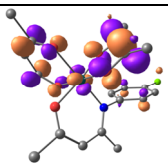
LUMO	LUMO+1	LUMO+2	LUMO+3

Table S18 Composition and energies of selected molecular orbitals of **2** (*S*=1/2)

MO	energy (eV)	% composition		
		Ru	L^-	$acac^-$
		α-spin		
HOMO–5	–6.237	11	39	50
HOMO–4	–6.0143	16	28	56
HOMO–3	–6.046	19	18	63
HOMO–2	–5.793	50	40	11
HOMO–1	–5.176	32	17	50
SOMO	–4.428	32	8	60
LUMO	–1.039	3	8	88
LUMO+1	–0.742	14	70	16
LUMO+2	–0.497	11	23	66
LUMO+3	–0.313	26	42	32
LUMO+4	0.129	6	89	5
LUMO+5	0.318	34	43	24
		β–spin		
HOMO–5	–6.363	8	49	43
HOMO–4	–6.186	10	31	59
HOMO–3	–6.041	15	37	49
HOMO–2	–5.904	19	20	60
HOMO–1	–5.631	51	40	9
SOMO	–5.084	38	19	43
LUMO	–2.488	32	62	7
LUMO+1	–1.024	3	7	91
LUMO+2	–0.561	9	23	68
LUMO+3	–0.336	21	65	14
LUMO+4	–0.192	22	54	55

α-spin			
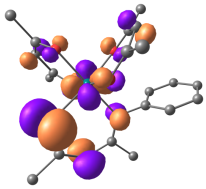	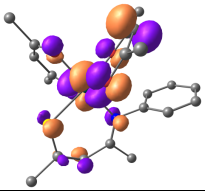	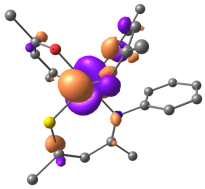	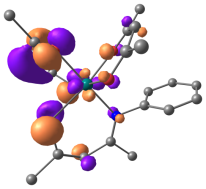
SOMO	HOMO–1	HOMO–2	HOMO–3
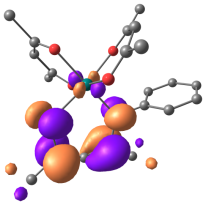	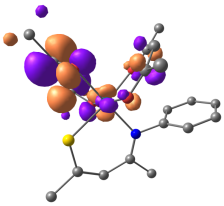	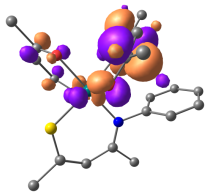	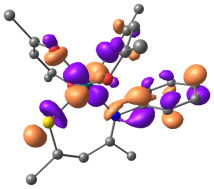
LUMO	LUMO+1	LUMO+2	LUMO+3
β-spin			
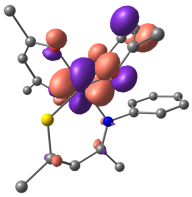	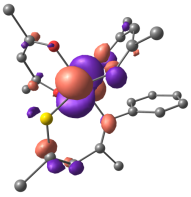	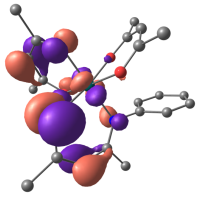	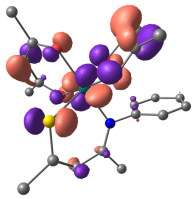
SOMO	HOMO–1	HOMO–2	HOMO–3
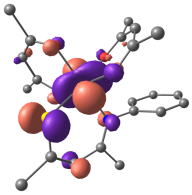	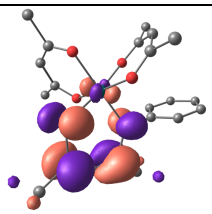	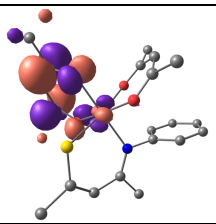	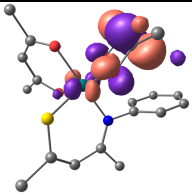
LUMO	LUMO+1	LUMO+2	LUMO+3

Table S19 Composition and energies of selected molecular orbitals of $\mathbf{2}^{+}$ (S=1)

MO	energy (eV)	% composition		
		Ru	L^{-}	$acac^{-}$
		α-spin		
HOMO–5	–10.339	7	30	63
HOMO–4	–10.070	43	42	15
HOMO–3	–9.676	2	21	77
HOMO–2	–9.608	4	71	25
HOMO–1	–9.469	3	88	9
HOMO	–8.498	29	62	9
LUMO	–4.821	35	24	41
LUMO+1	–4.549	20	32	48
LUMO+2	–4.455	9	34	57
LUMO+3	–.405	7	28	65
LUMO+4	–3.397	36	45	19
LUMO+5	–2.860	2	95	3
		β–spin		
HOMO–5	–10.074	17	48	35
HOMO–4	–9.827	21	38	41
HOMO–3	–9.715	41	49	11
HOMO–2	–9.614	6	64	29
HOMO–1	–9.508	7	25	68
HOMO	–9.421	8	75	17
LUMO	–7.761	45	19	36
LUMO+1	–6.418	30	63	7
LUMO+2	–4.580	25	16	59
LUMO+3	–4.444	3	5	92
LUMO+4	–4.060	15	75	10
LUMO+5	–3.234	33	49	18

α-spin			
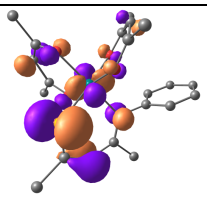	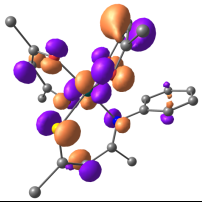	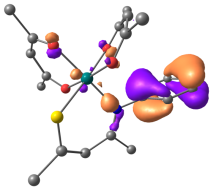	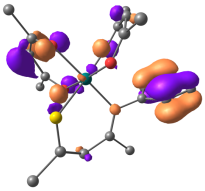
HOMO	HOMO–1	HOMO–2	HOMO–3
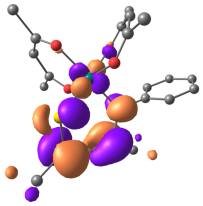	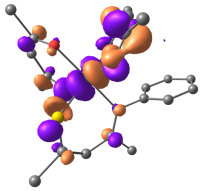	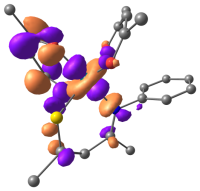	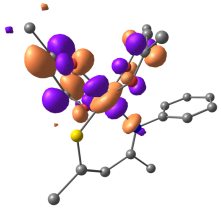
LUMO	LUMO+1	LUMO+2	LUMO+3
β-spin			
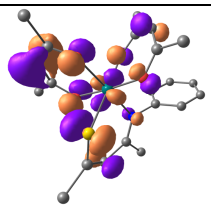	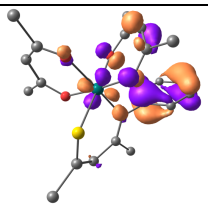	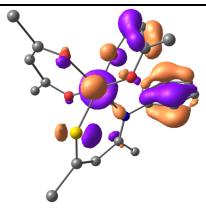	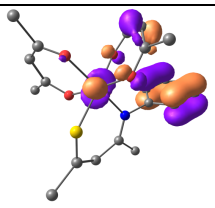
HOMO	HOMO–1	HOMO–2	HOMO–3
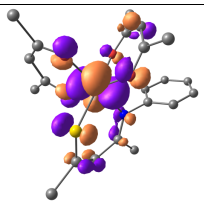	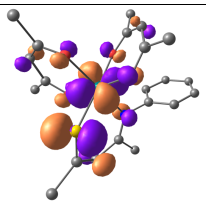	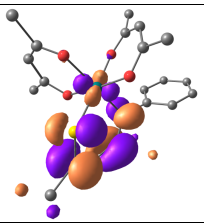	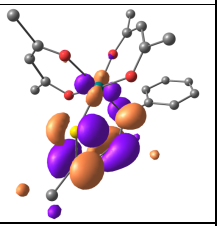
LUMO	LUMO+1	LUMO+2	LUMO+3

Table S20 Composition and energies of selected molecular orbitals of $\mathbf{2}^{-}$ (*S*=0)

MO	energy (eV)	% composition		
		Ru	L^{-}	$acac^{-}$
HOMO–5	–2.714	12	17	71
HOMO–4	–2.438	8	14	78
HOMO–3	–2.208	18	58	24
HOMO–2	–1.370	55	36	9
HOMO–1	–1.086	51	31	18
HOMO	0.314	31	63	7
LUMO	2.368	3	5	92
LUMO+1	2.763	4	5	91
LUMO+2	3.048	11	84	5
LUMO+3	3.190	2	92	5
LUMO+4	3.675	31	58	11
LUMO+5	4.080	61	11	28

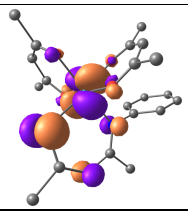	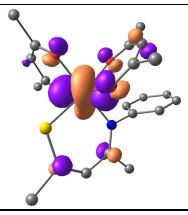	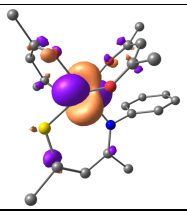	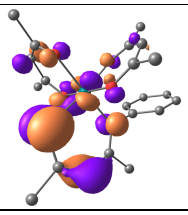
HOMO	HOMO–1	HOMO–2	HOMO–3
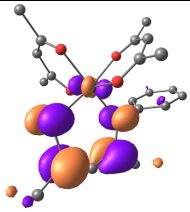	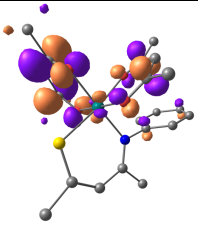	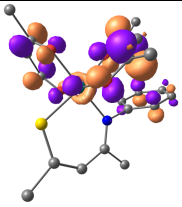	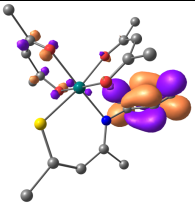
LUMO	LUMO+1	LUMO+2	LUMO+3

Table S21 Composition and energies of selected molecular orbitals of **3b** (*S*=1/2)

MO	energy (eV)	% composition		
		Ru	L^-	$acac^-$
		α-spin		
HOMO–5	–6.308	13	71	17
HOMO–4	–6.078	11	26	63
HOMO–3	–5.938	25	21	54
HOMO–2	–5.303	67	17	16
HOMO–1	–4.958	50	7	43
SOMO	–4.593	43	44	13
LUMO	–0.792	3	40	57
LUMO+1	–0.659	8	57	34
LUMO+2	–0.275	4	14	82
LUMO+3	–0.110	1	94	5
LUMO+4	– 0.054	10	73	17
LUMO+5	0.803	50	19	32
		β–spin		
HOMO–5	–6.275	7	79	14
HOMO–4	–6.233	15	23	62
HOMO–3	–5.880	25	22	53
HOMO–2	–5.777	10	49	41
HOMO–1	–5.022	67	17	15
SOMO	–4.743	58	9	33
LUMO	–1.986	53	34	13
LUMO+1	–0.762	3	22	75
LUMO+2	–0.468	15	66	18
LUMO+3	–0.220	6	18	76
LUMO+4	–0.105	1	96	4

α-spin			
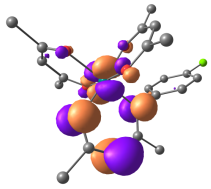	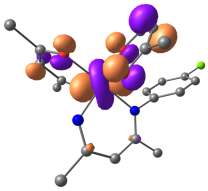	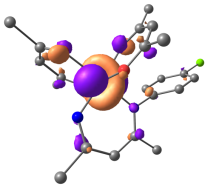	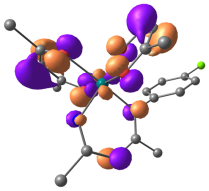
SOMO	HOMO−1	HOMO−2	HOMO−3
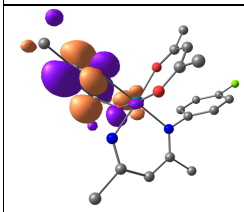	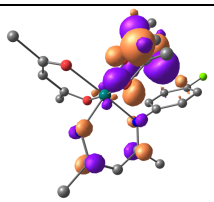	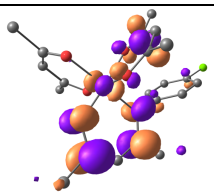	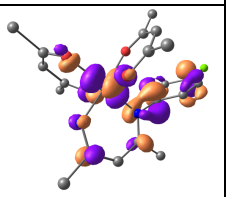
LUMO	LUMO+1	LUMO+2	LUMO+3
β-spin			
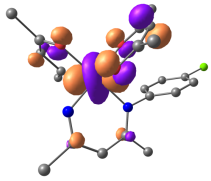	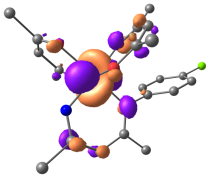	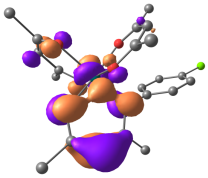	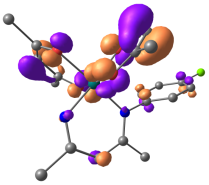
SOMO	HOMO−1	HOMO−2	HOMO−3
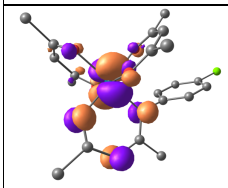	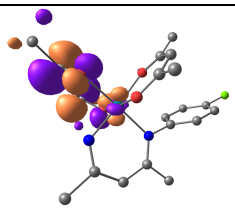	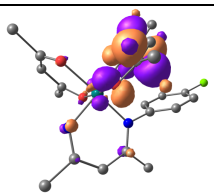	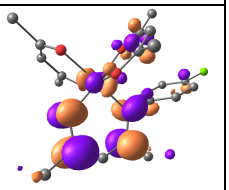
LUMO	LUMO+1	LUMO+2	LUMO+3

Table S22 Composition and energies of selected molecular orbitals of **3b**$^{+}$ (S=1)

MO	energy (eV)	% composition		
		Ru	L^-	$acac^-$
		α-spin		
HOMO–5	–10.205	7	77	16
HOMO–4	–10.068	59	23	19
HOMO–3	–9.815	4	20	76
HOMO–2	–9.542	12	15	72
HOMO–1	–9.371	3	91	5
HOMO	–8.962	32	50	18
LUMO	–4.713	4	93	3
LUMO+1	–4.548	27	12	61
LUMO+2	–4.260	17	9	74
LUMO+3	–4.130	18	7	75
LUMO+4	–3.378	32	48	20
LUMO+5	–3.234	1	96	3
		β–spin		
HOMO–5	–10.242	39	30	31
HOMO–4	–10.186	3	79	17
HOMO–3	–9.825	42	35	23
HOMO–2	–9.604	5	25	70
HOMO–1	–9.363	40	25	34
SOMO	–9.308	3	79	18
LUMO	–7.351	61	11	28
LUMO+1	–6.480	50	38	12
LUMO+2	–4.476	7	41	53
LUMO+3	–4.344	12	53	34
LUMO+4	–4.108	7	6	87

α-spin			
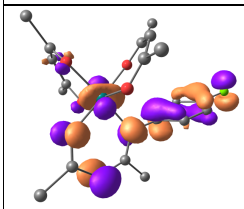	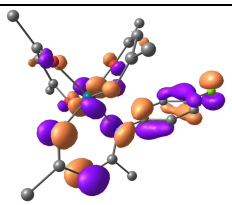	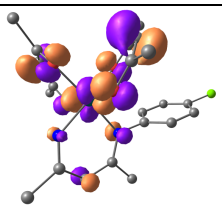	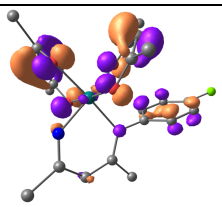
SOMO	HOMO−1	HOMO−2	HOMO−3
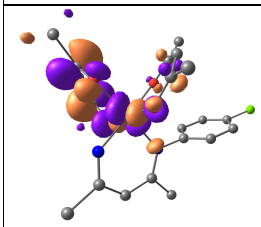	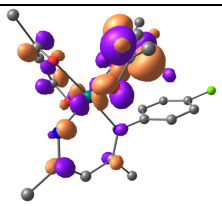	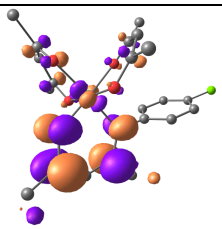	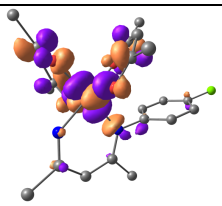
LUMO	LUMO+1	LUMO+2	LUMO+3
β-spin			
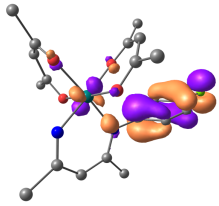	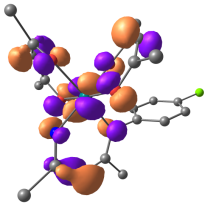	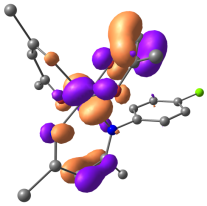	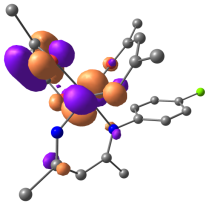
SOMO	HOMO−1	HOMO−2	HOMO−3
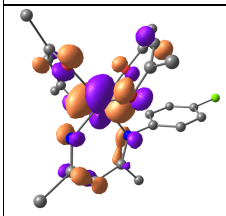	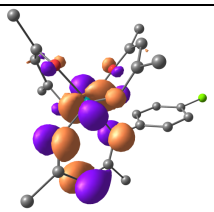	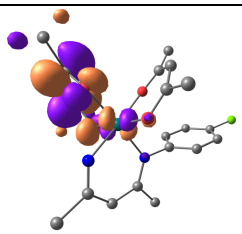	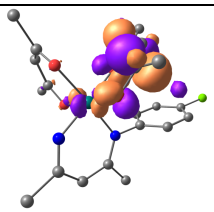
LUMO	LUMO+1	LUMO+2	LUMO+3

Table S23 Composition and energies of selected molecular orbitals of **3b**$^{-}$ (*S*=0)

MO	energy (eV)	% composition		
		Ru	L^{-}	$acac^{-}$
HOMO–5	–2.493	11	14	75
HOMO–4	–2.162	12	8	81
HOMO–3	–1.921	14	59	27
HOMO–2	–0.542	69	15	15
HOMO–1	–0.362	69	12	19
HOMO	0.559	53	34	13
LUMO	2.954	2	64	34
LUMO+1	2.976	3	50	48
LUMO+2	3.137	6	79	14
LUMO+3	3.389	8	12	80
LUMO+4	3.585	16	74	10
LUMO+5	3.890	31	62	7

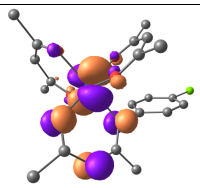	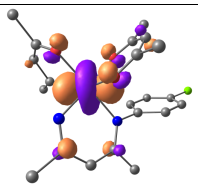	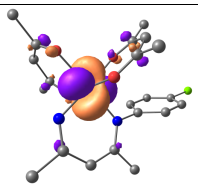	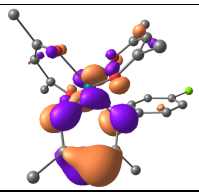
HOMO	HOMO–1	HOMO–2	HOMO–3
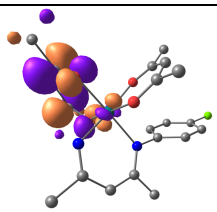	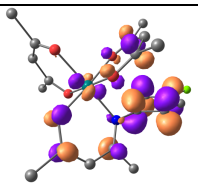	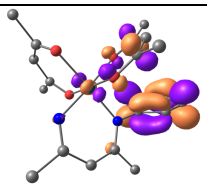	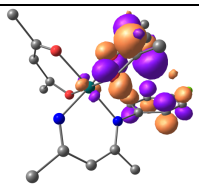
LUMO	LUMO+1	LUMO+2	LUMO+3